THEORETICAL INVESTIGATION OF CARBONYL SULFIDE CAPTURE BY AQUEOUS DIETHANOLAMINE SOLUTION

A MASTER'S THESIS

in

Chemical Engineering and Applied Chemistry

Atilim University

by

ABUBAKER MEFTAH HADIA

MAY 2017

THEORETICAL INVESTIGATION OF CARBONYL SULFIDE CAPTURE BY AQUEOUS DIETHANOLAMINE SOLUTION

A THESIS SUBMITTED TO

THE GRADUATE SCHOOL OF NATURAL AND APPLIED SCIENCES

OF

ATILIM UNIVERSITY

BY

ABUBAKER MEFTAH HADIA

IN PARTIAL FULFILLMENT OF THE REQUIREMENTS FOR THE DEGREE OF

MASTER OF SCIENCE

IN

THE DEPARTMENT OF CHEMICAL ENGINEERING AND APPLIED CHEMISTRY

MAY 2017

Approval of the Graduate School of Natural and Applied Sciences, Atılım University.

_____

Prof. Dr. Ibrahim Akman

Director

I certify that this thesis satisfies all the requirements as a thesis for the degree of Master of Science.

_____

Prof. Dr. Attilla Cihaner

Head of Department

This is to certify that we have read the thesis "theoretical investigation of carbonyl sulfide capture by aqueous diethanolamine solution" submitted by "ABUBAKER HADIA" and that in our opinion it is fully adequate, in scope and quality, as a thesis for the degree of Master of Science.

_____

Assist. Prof. Dr. Hakan Kayı

Supervisor

Examining Committee Members

Assoc. Prof. Dr. Murat Torun _____

Assoc. Prof. Dr. Seha Tirkeş _____

Assist. Prof. Dr. Hakan Kayi _____

Date: 12.05.2017

I declare and guarantee that all data, knowledge and information in this document has been obtained, processed and presented in accordance with academic rules and ethical conduct. Based on these rules and conduct, I have fully cited and referenced all material and results that are not original to this work.

Name, Last name: ABUBAKER HADIA

Signature:

ABSTRACT

THEORETICAL INVESTIGATION OF CARBONYL SULFIDE CAPTURE BY AQUEOUS DIETHANOLAMINE SOLUTION

Hadia, Abubaker

M.Sc., Chemical Engineering and Applied Chemistry
Supervisor: Assist. Prof. Dr. Hakan Kayı

May 2017, Pages: 79

Carbonyl sulfide (COS), an unwanted impurity, released with a variety of processing gases. Capturing of COS can be achieved with liquid absorbents.

Two different mechanisms are proposed in the literature for COS and diethanolamine (DEA) reaction, and both drive to a formation of thiocarbamate. The first mechanism is zwitterion intermediate mechanism, which takes two reaction steps. The first step is the forming of the zwitterion, and the second one is the deprotonation of the formed zwitterion. The second mechanism is termolecular mechanism in which a complex forms as intermediate in a single step reaction.

Four different termolecular reactions among COS, DEA and water were investigated through the quantum chemical calculations, and structural, energetic and thermochemical properties were revealed. Theoretical standard free energy of activation ($\Delta^{\ddagger}G^{\circ}$) and reaction ($\Delta G^{\circ}_{rxn}$), equilibrium constant (K_{eq}) and reaction rate constant (k) values for these four termolecular reactions were calculated. Density Functional Theory (DFT) was applied during the theoretical investigations of this study utilizing the B3LYP hybrid functional, and 6-311G(d) basis set.

In conclusion, calculated activation energy and reaction rate constant values obtained in this study were compared with the experimental data available in the literature, and

under the guidance of these findings, the most probable termolecular reaction mechanism for the COS capture by aqueous DEA solution was revealed.

Keywords**:** Carbonyl sulfide, Diethanolamine, DFT, Reaction mechanism, Absorption

ÖZ

KARBONİL SÜLFİTİN SULU DİETANOL AMİN ÇÖZELTİSİ İLE YAKALANMASININ TEORİK OLARAK İNCELENMESİ

Hadia, Abubaker

Yüksek Lisans: Kimya Mühendisliği ve Uygulamalı Kimya
Danışman: Yrd. Doç. Dr. Hakan Kayı

Mays 2017, 79 sayfa

Karbonil sülfit (COS), istenmeyen bir safsızlık olarak çeşitli proses gazlarıyla birlikte salınır. COS'u yakalamak, sıvı absorbentler ile başarılabilir.

COS ve dietanolamin (DEA) reaksiyonu için literatürde iki farklı mekanizma önerilmiş ve her ikisi de tiyokarbamat oluşumuna neden olmaktadır. Birinci mekanizma zvitteriyon (dipolar iyon) ara madde mekanizması olup, iki reaksiyon adımında gerçekleşir. İlk adım zvitteriyonun oluşturulması ve ikincisi oluşan zvitteriyodan proton giderme işlemidir. İkinci mekanizma, bir kompleksin bir tek aşamalı reaksiyonda ara madde olarak oluştuğu termoleküler mekanizmadır.

COS, DEA ve su arasındaki dört farklı termolekül reaksiyonu kuantum kimyasal hesaplamaları ile araştırılmış ve yapısal, enerjik ve termokimyasal özellikler ortaya konmuştur. Teorik standard serbest aktivasyon ($\Delta^{\ddagger}G^{\circ}$) ve reaksiyon enerjisi (ΔG°_{rxn}), denge sabiti (K_{eq}) ve bu dört termoleküler reaksiyon için reaksiyon hızı sabiti (k) değerleri hesaplanmıştır. Yoğunluk Fonksiyonel Teorisi (DFT), bu çalışmanın teorik araştırmaları sırasında B3LYP hibrid fonksiyoneli ve 6-311G (d) baz seti kullanılarak uygulanmıştır.

Sonuç olarak, bu çalışmada elde edilen hesaplanan aktivasyon enerjisi ve reaksiyon hızı sabit değerleri literatürde mevcut olan deneysel verilerle karşılaştırılmış ve bu bulguların rehberliği altında, sulu DEA çözeltisi ile COS yakalama için en olası termoleküler reaksiyon mekanizması ortaya çıkmıştır.

Anahtar kelimeler: Karbonil sülfit, Dietanolamin, DFT, Reaksiyon mekanizması, Absorpsiyon

Dedication

TO:

My Father, may ALLAH bless...

My Mother soul, may ALLAH be merceful with here...

My Wife and my Children, life is no meaning without you...

My Home Land, all the best...

ACKNOWLEDGMENTS

All thanks and gratitude to ALLAH Almighty, for all the graces that gave me.

Appreciation and gratitude to supervisor Assist. Prof. Dr. Hakan Kayı and co-supervisor Prof. Dr. Erdoğan Alper for providing advice, guidance, and assistance throughout the research period, I am really grateful to you.

Thanks for all academic staff in the Chemical Engineering and Applied Chemistry department of Atilim University.

My special thanks and appreciation to all of my family, my father, my wife and kids who have spared no effort to help and encourage me through care and love, may ALLAH bless and protect you, and being merciful for the soul of mom in her grave.

TABLE OF CONTENTS

LIST OF TABLES

LIST OF FIGURES

LIST OF ABBREVIATIONS

LPG	-	Liquefied Petroleum Gas, Natural Gas
RSH	-	Thiol
DEA	-	Diethanolamine
B	-	BASE
DFT	-	Density Function Theory
NMR	-	Nuclear Magnetic Resonance
HF-SCF	-	Hartree-Fock Self-Consistent Field Method
PES	-	Potential Energy Surface Concept
R	-	Position
T	-	Time
Ψ	-	Wave Function
H	-	Hamiltonian Operator
E	-	Energy
E_{el}	-	Electronic Energy Eigenvalue
T	-	kinetic energy
U	-	Electron–electron interaction energy
V	-	Potential energy
N	-	Number of electrons
Z	-	Atomic number
V_{ext}	-	External potential
ρ	-	Electron Density
E_{XC}	-	Exchange correlation energy
AO	-	Atomic Orbital
MO	-	Molecular orbital
HK	-	Hohenberg and Kohn
ϕKS	-	Kohn–Sham orbital
LDA	-	Local Density Approximation
LCAO	-	Linear Combination of Atomic Orbitals
STO	-	Slater Type Orbitals
GTO	-	Gaussian Type Orbitals
B3LYP	-	Becke 3-Term Correlation Functional; Lee, Yang, And Parr Functional
GGA	-	Generalized Gradient Approximation
IR	-	Infra-red
Ea	-	Activation energy
ΔErxn	-	Change in internal energy of the reaction
Keq	-	Equilibrium constant
k , kapp	-	Reaction rate constant
$\Delta^{\ddagger}G^{\circ}$	-	Standard free energy of activation

$\Delta G°_{rxn}$	-	standard free energy of reactıon
DWOCS	-	First mechanism: DEA(H of N)+Water+O=C=S
DWSCO	-	Second mechanism: DEA(H of N)+Water+S=C=O
WDOCS	-	Third mechanism: DEA(H of OH)+Water+O=C=S
WDSCO	-	Fourth mechanism: DEA(H of OH)+Water+S=C=O

CHAPTER 1

INTRODUCTION

Carbonyl sulfide (COS) whose chemical structure is shown in figure 1.1, is an unwanted impurity released along with a variety of process gases such as carbon dioxide (CO_2), hydrogen sulfide (H_2S) and carbon disulfide (CS_2).

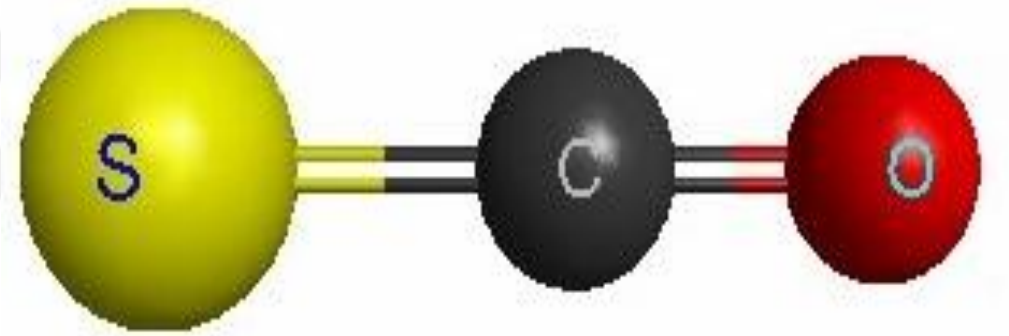

Figure 1.1 Carbonyl sulfide structure from B3LYP/6-311G(d) calculations.

Chemical engineers pay attention to the presence of COS in industrial gas streams, and give more importance to the new industrial case which is the existence and occurring of COS naturally in liquefied petroleum gas (LPG).

To follow the pollution regulations and to meet the strict environmental requirements in gas delivery industries, the impurities in gas streams which are toxic and have corrosive abilities should be cleaned, either by chemically recycling to another process or any other suitable way not to affect environment.

In Claus process which is the most important gas desulfurizing process, hydrogen sulfide is oxidized at a high temperature (around 850 ºC) to yield elemental sulfur.

Carbon dioxide is also formed in this combustion. Hydrogen sulfide reacts with this carbon dioxide, and carbonyl sulfide is mainly being formed.

The formed carbonyl sulfide in the Claus process, considered as a polluting byproduct, because it goes into hydrolysis, and this hydrolysis process yields again hydrogen sulfide and carbon dioxide [1].

Hydrolysis of carbonyl sulfide has known to be one of the reasons of corrosion and insufficiency in the LPG industry. Also, it causes environmental issues which become more and more of the concern recently.

Generally, carbon dioxide and hydrogen sulfide hydrolysis are easier than carbonyl sulfide. So, it is necessary to have further costly processes, which have to be done for the removal of carbonyl sulfide [2].

The removal of the sulfur compounds coming out with natural and synthesis gases considered as an important operation in industrial processes, because of their undesirable properties such as their capability of damaging the equipment, and their toxic properties.

Hydrogen sulfide is the most popular sulfur component in natural gas. Some various quantities of carbonyl sulfide and carbon disulfide are often present depending on the natural gas type and geographical area. These sulfur species are corrosive to pipelines and other different processing equipment; they poison the catalysts and have a high toxicity. Consequently, strict regulations prescribed for transportation in pipelines limiting the concentrations of those sulfur compounds content in natural gas and other crude oil pipelines, to be often under 4 ppm [3].

Natural gas is getting more and more importance worldwide every day. After extraction, natural gas, cannot be transported or used commercially. First, it must be treated to remove acid gases, such as carbon dioxide, hydrogen sulfide and other contaminants such as carbonyl sulfide, carbon disulfide, and mercaptans (RSH) [4].

The carbonyl sulfide is naturally found in petroleum fractions, and it causes some troubles in some petrochemical processes. As carbonyl sulfide and propane (C_3H_8) are similar in boiling point temperatures (-44.5 °C for C_3H_8, -50.2 °C for COS), after the extraction, the propane fraction may contain 90% of the petrochemical carbonyl sulfide. Other trouble is that, due to the saturation of natural gas with water, the carbonyl sulfide going through hydrolysis with this water to produce hydrogen sulfide at the well head and before transportation [5].

The carbon dioxide, as a Greenhouse gas, is considered as a main reason for global warming, the gases containing sulfur as hydrogen sulfide and carbonyl sulfide are considered as toxicants. So, the release limits of the refinery discharged gases are exposed to more and more strict regulations. These gases should be removed from the natural gas before transportation because of their ability to damage the pipelines as well as the transportation equipment [6].

1.1 ENVIRONMENTAL ISSUES

Carbonyl sulfide is a small component of Earth's environment [7], being originated from different sources, such as emissions rising up from volcanoes and warm water resources, and different chemical and biochemical processes in soils and sediments [8].

Carbonyl sulfide is considered as a reason in forming of sulfur dioxide in the atmosphere, and this possibly may have an effect on global climate change [9].

The lifetime of carbonyl sulfide, after taking into consideration its oxidation by the hydroxyl ion (OH), is more than nine years, and due to its chemical stability, its lifetime in the atmosphere is near four years [10, 11].

The surface ocean is also a natural source of sulfur gases. Emissions coming out from the ocean represent about one-third of the total carbonyl sulfide emitted to the atmosphere [12].

The refineries and different industrial plants in the energy sector are also considered as a source of carbonyl sulfide and other sulfur compounds, which have a serious effect on the environment.

1.2 HEALTH AND SAFETY

Carbonyl sulfide has the a limited ability to go through hydrolysis and hydrogen sulfide is produced from this process, because of this hydrolysis, carbonyl sulfide can be classified as an irritant substance to the eyes, skin, respiratory system and it causes sneezing and cough [13].

Carbonyl sulfide classified by Houriet and Louvier [14] as a class II toxicity substance. The toxicity value of carbonyl sulfide according to this classification is 23 ppm (mass/mass) for mammals.

1.3 CARBONYL SULFIDE REMOVAL

There must be a work to be done on removing sulfur compounds from those industries which involved in COS production to follow strict environmental standards and reaching specifications distributed by gas transport industries.

Capturing of carbonyl sulfide from mixtures of gases is an important industrial operation, and can be achieved by treating the COS with liquid absorbents [15].

The removal of various sulfur compounds, mostly done by a process of chemical absorption through solvents. Alkanolamines are the most common solvents used in this process [4].

The alkanolamines such as diethanolamine (DEA) is typical solvent for removing exhausted gases such as carbon dioxide and carbonyl sulfide. Diethanolamine is one of the most commonly used solvents nowadays. Diethanolamine can be considered as an indicator that other solvents can be compared with [16]. Diethanolamine molecule is shown in Figure 1.2.

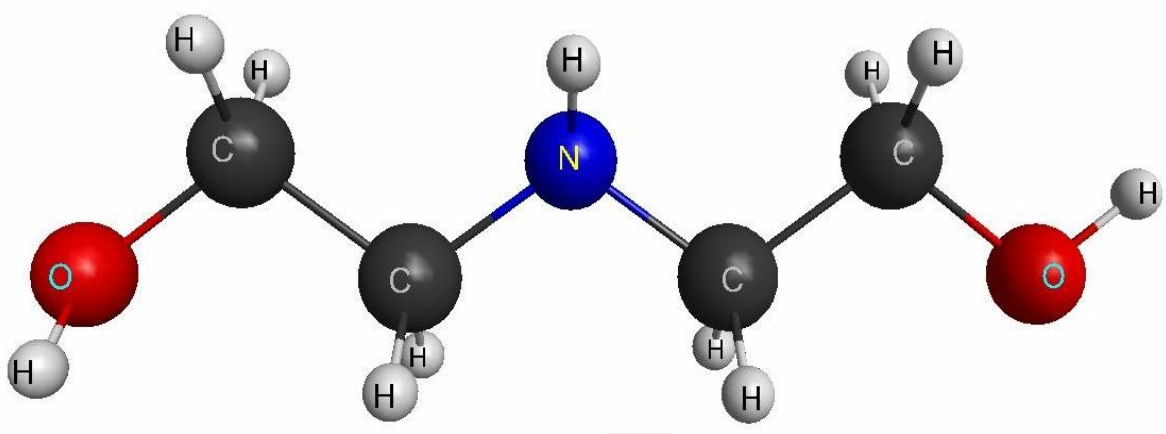

Figure 1.2 Diethanolamine structure from B3LYP/6-311G(d) calculations.

Amines are classified in three groups to be primary, secondary and tertiary amines, according to the number of carbon atoms bonded to the nitrogen atom of amine group.

A lot of different alkanolamines, other than diethanolamine (DEA) are also used to remove sulfur species such as monoethanolamine (MEA) and di-isopropanolamine (DIPA) [15].

With respect to mass transfer, hydrogen sulfide reacts with alkanolamines instantaneously, while the carbon dioxide and alkanolamines reaction considered as a finite rate reaction. The selectivity of hydrogen sulfide, from other gases, can be processed when using an alkanolamine that comparatively reacts slowly with carbon dioxide [17].

The reaction kinetics of the carbonyl sulfide and carbon dioxide with primary and/or secondary alkanolamines was studied by Sharma [15], and it was found that carbonyl sulfide reacts with these alkanolamines 100 times slower than the reaction of carbon dioxide with them.

Because COS reacts with alkanolamines slower than carbon dioxide and hydrogen sulfide, usually, a decrease in carbonyl sulfide absorbing ability occurs with the selectivity increase of hydrogen sulfide. Thus, the decrease of carbonyl sulfide removal

limits the total sulfur selectivity because the target of the process here is a total sulfur removal [17].

An intensive understanding of the kinetics and mechanisms of the reaction between alkanolamines and carbonyl sulfide is needed to reach and achieve a good enough design of gas treatment plants [17].

1.4 LITERATURE REVIEW

Although there are a lot of studies in carbonyl sulfide reaction with alkanolamines, the kinetics data published have not really satisfied the researchers, and a few works [3, 4, 6, 15, 17, 18] studied the kinetics of COS absorption by aqueous DEA.

Sharma [15] studied the kinetics of carbonyl sulfide absorption by using different primary and secondary alkanolamines. The limitation in this study was that the only temperature degree used was 298 K, as well as using only one concentration of amine which was 1000 $mol.m^{-3}$. Sharma proposed that the reaction mechanisms of carbonyl sulfide with primary and secondary alkanolamines were analogous to that of carbon dioxide via a zwitterion mechanism.

Singh and Bullin [19] studied the carbonyl sulfide absorption in an aqueous solution of diglycolamine (DGA). In this study, they simulated the reactor column absorption stage. The temperature in this study ranged from 307 K to 322 K, and concentration of DGA varied from 3220 $mol.m^{-3}$ to 5630 $mol.m^{-3}$.

Al-Ghawas et al [20] used a wetted sphere apparatus as one of the kinetic experiments. They published some data for diffusion coefficients and carbonyl sulfide Henry's constant in aqueous solutions of methyl diethanolamine (MDEA). The temperature ranged from 298 K to 313 K, and the concentrations of MDEA ranged from 1259 $mol.m^{-3}$ to 2599 $mol.m^{-3}$.

Hinderaker and Sandall [3] provided kinetics data for absorption of carbonyl sulfide in aqueous dietanolamine solution with a concentration of 5 to 25 wt %, under

temperature ranges between 298 K and 348 K. They proved the validation of the analogy of COS and nitrous oxide (N_2O) by carrying out measurements on carbonyl sulfide and nitros oxide (COS-N_2O) solubility and diffusivity in polyethyleneglycol aqueous solution at a temperature of 298 K. Also, they found that the deprotonation of the zwitterion is the limiting step for the reaction of carbonyl sulfide absorption in aqueous diethanolamine solution.

Little et al [17] also contributed to provide carbonyl sulfide kinetics data with primary and secondary alkanolamines. They obtained them using a stirred cell reactor, in a temperature range between 283 K and 333 K. In order to determine the carbonyl sulfide physicochemical parameters, the authors also used a carbonyl COS-N_2O analogy. They concluded that the mechanism of the reaction of carbonyl sulfide with primary and secondary alkanolamines is zwitterion mechanism, and the zwitterion deprotonation is the limiting step in the reaction.

Little et al [21, 22] also studied the COS absorption with the aqueous solutions of tertiary alkanolamines in a stirred cell reactor. All experiment temperatures were fixed at 303 K, except the MDEA aqueous solutions experiment in which temperatures ranged between 293 K to 323 K. The concentrations of alkanolamines ranged between 153 $mol.m^{-3}$ to 1011 $mol.m^{-3}$. A numerically solved absorption model based on Higbie's penetration theory used in part 2 of this work [22] to explain absorption experiments and calculate absorption rates proceeded in part 1 of this work [21]. Experimental and calculated absorption rates agreed reasonably well at relatively low amine concentrations but deviated increasingly with increasing amine concentration.

A study of Alper and Bouhamra [23] confirmed that the reaction order for COS absorption in akanolamines increases from first to second order as alkanolmine concentrations increase.

It is noted after this review that the removal of carbonyl sulfide needs more detailed understanding of the reaction mechanisms and kinetics when it is absorbed in alkanolamines.

1.5 REACTION MECHANISM

The kinetics and reaction mechanisms between gas stream components and aqueous alkanolamine solution, got a large importance because the selective removal of each component from the gas stream is desired. The knowledge of these properties allow designers to choose suitable absorbent and appropriate mechanism to achieve the target which is the selective removal of each contaminant.

Gas streams removal techniques, which use aqueous alkanolamine solutions, have to be able to deal with the small quantities of COS present in gas streams with large amounts of CO_2 and H_2S [18].

Carbonyl sulfide reacts slower than carbon dioxide with amines, which means may be low total sulfur removal if didn't use the convenient reactive amine for the gas stream. Thus, such kinetics and mechanism studies are needed to achieve the target of COS removal [18].

In carbonyl sulfide case, it was shown by Littel et al and Alper [17, 24] that the mechanism of zwitterion intermediate can drive to a formation of thiocarbamate, but, for all the studied amines, the reaction was completely or mostly dependent on the deprotonation rate of the zwitterion.

Alper and Bouhamra [18] experimentally studied the reaction of carbonyl sulfide in aqueous primary and secondary amine. They use four industrially important amines, DGA, DEA, DIPA and morpholine. The temperature was between 278 K and 298 K. In this experiment stopped-flow technique was used. Their findings confirmed that the reaction of carbonyl sulfide in aqueous solutions of primary and secondary amines is a single step termolecular reaction involving a water or another amine molecule.

It is known that ethylenediamine and diethylenetriamine react fast with carbon dioxide [25]. According to this, the deprotonation of the zwitterion won't participate in the rate of CO_2-amine reactions.

The similarity of the structure of carbon dioxide and carbonyl sulfide, as linear compounds, leads to a similarity in their reactions [18]. This assumption used by researchers in this field to build their theories, and then support this assumption with data extracted from experiments. For example, Sharma [15], assumed a formation of thiocarbamate from COS-amine reaction following findings those indicate CO_2-amine forms a carbamate.

The reactions between carbonyl sulfide and primary (RNH_2) or secondary (R_2NH) amines, are analogous to their reaction with carbon dioxide, and the zwitterion mechanism can be given as [17, 18]:

$$COS + R_2NH \underset{k_{-1}}{\overset{k_2}{\rightleftharpoons}} R_2NH^+COS^- \quad (1)$$

$$R_2NH^+COS^- + B \underset{k_{-B}}{\overset{k_B}{\rightleftharpoons}} R_2NCOS^- + BH^+ \quad (2)$$

Equation (1) illustrates the forming of the zwitterion intermediate, while Equation (2) illustrates the reaction of the zwitterion deprotonation. The thiocarbamate which results from the deprotonation of the zwitterion can be obtained by any base (B) exist in the solution, like amine, alcohol and water, or a mixture of them. Some publications agreed with this mechanism [17, 18]. Proposing that this zwitterion is a reactive medium, its concentration is weak and steady state is reached fast. The rate of reaction of carbonyl sulfide is given by [6]:

$$r = \frac{k_2[COS][R_2NH]}{\frac{1+k_{-1}}{k_B[B]}} \quad (3)$$

or

$$r = k_{app}[COS] \quad (4)$$

Crooks and Donnellan [26] proposed another mechanism for the reaction between carbon dioxide and systems of aqueous alkanolamines. According to this mechanism, it is a termolecular and single step reaction.

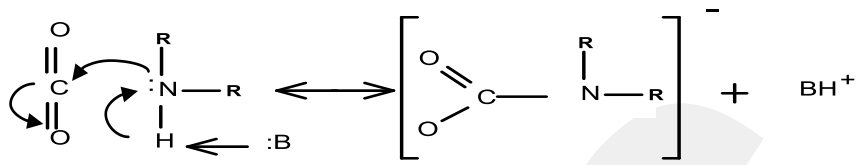

(5)

According to Alper and Bouhamra [18], the reaction of carbonyl sulfide with primary and secondary alkanolamines follows this termolecular mechanism which results with thiocarbamate formation.

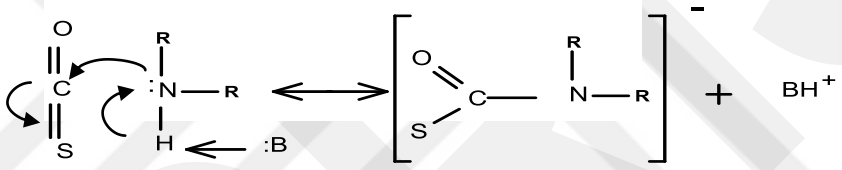

(6)

Termolecular mechanism proposes that the reaction between the amine and one molecule of COS and one molecule of the base, occurs at the same time in a single step, yielding an intermediate of a complex.

The mechanisms suggested in equations (5) and (6) can be considered as similar mechanism, i.e. termolecular mechanism [18].

The termolecular mechanism here can be exemplified as [6]:

$$COS + R_2NH \ldots B \leftrightarrow R_2NCOS^{-} \ldots BH^{+} \qquad (7)$$

The complex cleaves to go back forming the reactants molecules, where a small part of this complex again reacts with an other alkanolamine or water molecule to produce ionic products. The value of k_{app} is given by [6, 18]:

$$k_{app} = k_{H_2O}[R_2NH][H_2O] + k_{R_2NH}[R_2NH]^2 \qquad (8)$$

By looking at the termolecular mechanism suggested in equations (5) and (6), it can be observed that the formation of the bond and the transfer of the proton towards the base happen simultaneously. This transformation occurs in a single step, carrying the reaction to the 3rd order. Termolecular mechanism in equations (5) and (6) can be clearly noticed that it differs when compared with the mechanism occur by zwitterion as suggested in equations (1) and (2) [27].

As the aqueous alkanolmines are the best applicable proven technology for CO_2 and COS capture and removal, nowadays efforts are beeing made to develop this technology in order to get more knowledge about it, and to use in large scale to reduce acid-gas emissions.

The mechanism of the reaction is still argumentative. In fact, it needs more clarifications which can drive to additional improvements in optimizing the design for gas capture techniques.

In this thesis, a computational chemistry methodology, density functional theory at the B3LYP/6-311G(d) level is utilized to investigate and reveal the reaction kinetics of the carbonyl sulfide absorption with aqueous diethanolamine solution, which is defined as the COS/DEA/Water system.

The termolecular COS/DEA/Water mechanism was applied in this study, taking into account of four types of proton transfer:

Reaction System 1) DWOCS: transfer of proton of Nitrogen to water and transfer of proton from water to the oxygen atom of O=C=S.

Reaction System 2) DWSCO: transfer of proton of Nitrogen to water and transfer of proton from water to the sulfur atom of S=C=O

Reaction System 3) WDOCS: transfer of proton of -OH group in amine to water and transfer of proton from water to the oxygen atom of O=C=S

Reaction System 4) WDSCO: transfer of proton of -OH group in amine to water and transfer of proton from water to the sulfur atom of S=C=O.

CHAPTER 2

METHODOLOGY

COMPUTATIONAL CHEMISTRY

2.1 INTRODUCTION

For some decades, a lot of alkanolamines studied as solvents for CO_2 and COS absorption. There has been a satisfied illustration for the chemistry, but on the other hand, there are some shortage or limited clarification of the structure of the molecules and the chemical equilibrium [28].

A question can always be asked, how to proof a theory or a law by a theoretical experiment, or by calculating the experimental problems within a theoretical system?

The answering of this question will lead us to the computational modeling of theories or laws [29].

In applied chemistry and chemical engineering science, the applied experiments, sometimes, needs some extra procedures and costs or trial and error methods as well as the risk accompanying with them. All these facts trend to simulate or model systems to achieve the best performance in the studied system.

Why to use computers for molecular modeling?

The purpose of preparing a model is almost to be specifically applied in a definite area which can be named as chemical space [29].

This technique, i.e. molecular modeling, allows researchers to discover deep in chemistry molecules, with the following advantages [30]:

- More likable alternated method than the classically drawn lines.
- These models seem to be similar to the actual molecule.
- You can rotate this computer model and see it from various angles.
- The positions of the atoms can be shown in various ways.
- In case of wrong drawings, the model can be corrected by the data saved in the software.
- Modeling deals better than hand drawings of unstable molecules, when need to express delocalized charges and reactions at transition state.
- Various properties like attractive forces, energies, spectrum and frequency properties can be displayed and predicted by molecular modeling.

Thus, molecular modeling by computer is more than a computer screen showing a structure, it is astudy, imagination, optimization and research or investigation of the chemical phenomenon.

There is a confirmed relation between the improvement of the theories in chemistry science and the improvement of computation software and hardware. Sometimes difficulties in testing a theory originate from the disabilities in solving its equations. Improvement of the computational techniques can allow those theories to be applicable, even if they are with more increasing complex systems [29].

The object of a theory is achieving the generality. Many theories can be applied at macroscopic systems, but they couldn't be applicable to very small systems. Quantum theory, for example, has intractable equations, but it is the most ideal for small systems. The model can simplify the quantum calculations into general theory [29].

The model is almost designed to be applied on a definite volume which can be called chemical space. It is almost involving calculations for simplifying the approximations to generalize a theory for extending its utilizations [29].

Theoretical chemistry tries to illustrate [31]:

- Geometries and structure properties of molecules.
- Some properties such as wave function, energies, IR vibrations, polarization, dipole moment, and Nuclear Magnetic Resonance (NMR), etc.
- The interaction between different molecules and potential energy surface of reactions.

Computational chemistry is fastly rising up as one of the theoretical chemistry branches, in which the main focus is to solve the chemical problems by mean of the calculations [31].

One of computational chemistry's great effects lies in its capability to create data and wave function analysis, for instance, this data may provide us with more understanding to get insight and more highlights about a phenomenon. Then we can justify the behavior of many different groups of molecules [31].

The computational chemistry field can be considered as old and young at the same time. The old consideration coming from that it was founded since the development of quantum mechanics in the beginning of the twentieth century. On the other side, it is still young because no technology other than digital computers and software has developed that fast in the last two decades [29].

As two particle system can follow mathematical procedures, and be analytically solved, multi-particle systems can't follow these analytical methods. There are many computational methods which can solve this multi-particle systems problems, and can obtain an approximated solutions [31].

Before going deeper in our computational chemistry methodology, and in order to understand more about it, one needs to take a look at the background of particles theories.

2.2 QUANTUM MECHANICS

The calculations that possibly done by quantum mechanics can be employed to clarify a reaction mechanism, and highlight these mechanisms [28].

Quantum mechanics presents a chance of calculating a lot of chemical properties, even with some or no experimental data in hand. Over the years, calculations of quantum mechanics improved in computational chemistry applications, and nowadays these calculations applied successfully in research and guess of the structure of molecules, mechanisms of reactions, thermodynamics and spectroscopic characterizations of studied systems [28].

The dynamical equation is mathematically expressed in terms of particle's mass and velocity, which can be split into four regimes as shown in figure 2.1.

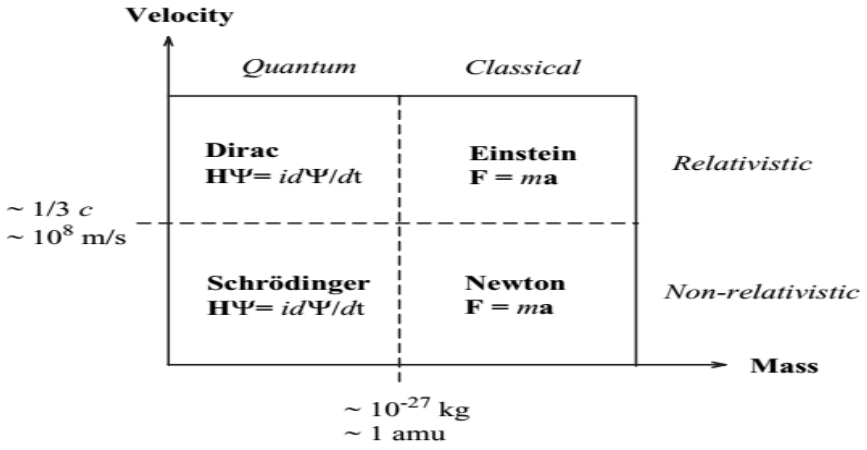

Figure 2.1 Domains of dynamical equations [31].

The quantum mechanics differs from the classical one because it can be only explained in a probabilistic ways or approximations, while classic mechanics is considered as deterministic [31].

In the deterministic mechanics (classical one), Newton's equation is integrated, and according to that, one can expect the place of particles at a definite time. For instance,

this makes the time and location prediction of the solar eclipses before they happen, for many centuries with high accuracy. But, in quantum mechanics, a certain place and time can be only calculated probabilistically. The probability function is given as the square of a wave function.

$$P\ (\mathbf{r}, t)\ =\ \Psi^2\ (\mathbf{r}, t) \qquad (1)$$

where **r** is the position, *t* is time, and wave function Ψ can be calculated either by solving non-relativistic Schrödinger equation or by solving relativistic Dirac equation (figure 2.1) [31].

The time independent Schrödinger equation, i.e. electronic Schrödinger equation for *N*-electron atomic or molecular system can be simply written as:

$$H\Psi = E\Psi \qquad (2)$$

The Hamilton operator (*H*) made up of contributions of potential and kinetic energies, those can be called electronic energy [32].

In quantum chemical approaches, the target is the approximation solution of the time independent non-relativistic Schrödinger equation:

$$H\ \Psi_i(X_1, X_2, \dots, X_N, R_1, R_2, \dots, R_M) = E_i\Psi_i(X_1, X_2, \dots, X_N, R_1, R_2, \dots, R_M) \qquad (3)$$

H is the Hamiltonian operator of a molecular system composed of *M* nuclei and *N* electrons. The wave function Ψ_i has all information can possibly known about the studied quantum system, it stands for the *i*'th state of the system which depends on X_N the spatial and spin coordinates, and X_M the spatial coordinates of the nuclei. E_i is the numerical value of the energy of the state described by Ψ_i. *H* also is a differential operator represents the total energy, as illustrates in this next equation with five terms:

$$H = -\frac{1}{2}\sum_{i=1}^{N}\nabla_i^2 - \frac{1}{2}\sum_{A=1}^{M}\frac{1}{M_A}\nabla_A^2 - \sum_{i=1}^{N}\sum_{A=1}^{M}\frac{Z_A}{r_{iA}} + \sum_{i=1}^{N}\sum_{j>i}^{N}\frac{1}{r_{ij}} + \sum_{A=1}^{M}\sum_{B>A}^{M}\frac{Z_A Z_{AB}}{R_{AB}} \quad (4)$$

A and *B* run over the *M* nuclei, *i* and *j* denote the *N* electrons in the system, M_A is the mass of nucleus and *A*, r, and *R* are the distances between the particles. The first term describes kinetic energy of the electrons (electronic kinetic enenrgy), second one describes nuclei (nuclear kinetic energy), and the rest of the equation describes the potential energy part of the Hamiltonian, where the third term represents the attractive electrostatic interaction between the nuclei and the electrons, and fourth and fifth describe the repulsive potential due to the electron-electron and nucleus-nucleus interactions respectively [33].

Variational principle states that the energy determined from any approximate wave function will always be greater than or equal the exact energy [31].

Variational principle is important principle in all quantum chemical applications. It is recall from standard quantum mechanics that the expected value of an observable represented by operator *O* using any wave function Ψ_{trial} is given by [33]:

$$\langle O \rangle = \int \dots \int \Psi^*_{trial} \; O \; \Psi_{trial} \; \mathrm{d}\vec{\mathrm{x}}_1 \mathrm{d}\vec{\mathrm{x}}_1 \dots \mathrm{d}\vec{\mathrm{x}}_1 \equiv \langle \Psi_{trial} | O | \Psi_{trial} \rangle \quad (5)$$

Although Schrödinger and Dirac equations in Figure 2.1 seem to be similar, they differ according to the form of the factor *H*. For small mass particles like electrons, quantum mechanics time-dependent Schrödinger equation is employed [31].

$$H\Psi \; = \; i \frac{\partial \Psi}{\partial t} \quad (6)$$

The Hamiltonian operator here is the sum of the operators of kinetic energy (*T*) and potential energy (*V*).

$$H_{Schrodinger} \; = T + \; V \quad (7)$$

And the solution of Schrödinger equation yields equation (1), which gives the probability of observe a particle at a position **r** and time *t*.

For light particles which move at a significant part of the light speed, the Dirac equation is employed.

$$H\Psi = i\frac{\partial \Psi}{\partial t} \quad (8)$$

The Hamiltonian operator here is more complicated.

$$H_{Dirac} = (c\boldsymbol{\alpha}.\mathbf{p} + \boldsymbol{\beta}mc^2) + V \quad (9)$$

The **α** and **β** are 4 × 4 matrices, and relativistic wave function has four components called large and small components, each component has α and β spin functions which are different than **α** and **β** matrices. Wave function here has two parts, electronic part which described by large component and positronic part which described by small component, then **α** and **β** matrices couple the components. In the limit c→ ∞, Dirac equation reduces to Schrödinger equation, also, large components of the wave function reduced to α and β spin orbitals in Schrödinger picture.[31].

Wave function describes the system's physical properties. Definitely, it applies the factors (operators) in quantum mechanics related to the physical property to be studied. Then it permits the expectations of the probabilities allowing the system to display a specific value/values for that physical property [29].

Molecules and atoms are heavier than electrons and behave basically like classical particles. On the other hand, electrons are lighter and expressed by quantum mechanics, also particles of light have wave and particle properties, those can only be expressed by quantum mechanics [31].

It is not easy to define simply or to give a physical explanation of a wave function. Also it is impossible to derive a wave function directly [16].

Assuming that one want to solve the electronic Schrödinger equation for a molecule. Then each electron function is considered as molecular orbitals (MO) [31].

Electrons are described with aspin quantum number, and same quantum number can't be given to two electrons, then a molecular orbital is fixed for two electrons in opposite spin [16].

Schrödinger equation is an accurate postulate, it is so complicated that the biggest system it can solve analytically is a hydrogen atom. In this case, Dirac and others did a lot of approximations for the possibility of calculating the multi-particle system [16].

Some of these approximations are briefly summarized in the next sections.

2.3 AB INITIO COMPUTATION METHODS

Ab Initio methods utilize only mathematical approximations to solve Schrödinger equation.

2.3.1 Born-Oppenheimer Approximation

As our study deals with multi-molecular systems theoretically, indeed, stating the expression of the wave function of these systems is so complicated because movements of the species affected by attraction and repulsion forces among them. This means, these particles can't travel independently of each other [29].

In a system, where nuclei and electrons are exist, it's known that the nuclei move much slower than the electrons because they are heavier than electrons. So it is suitable to separate these two movements and calculate electronic energies in the fixed positions of nuclei [29].

This leads to consider that the kinetic energy of nucleus is taken independent of the electrons, and then potential energy of electron-nuclear attraction is eliminated. And at this point the potential energy of nuclear-nuclear repulsion becomes constant [29].

Born-Oppenheimer approximation is also called the clamped nuclei approximation because it's assumed that the electrons are moving in a field of fixed nuclei, and the complete H in eq. (4) reduces to electronic Hamiltonian H_{elec} [33].

$$H_{elec} = -\frac{1}{2}\sum_{i=1}^{N}\nabla_i^2 - \sum_{i=1}^{N}\sum_{A=1}^{M}\frac{Z_A}{r_{iA}} + \sum_{i=1}^{N}\sum_{j>i}^{N}\frac{1}{r_{ij}} = T + V_{Ne} + V_{ee} \qquad (10)$$

Solution of Schrödinger equation with electronic Hamiltonian, H_{elec}, is the electronic wave function Ψ_{elec} and the electronic energy E_{elec} [33].

$$H_{elec}\ \Psi_{elec} = E_{elec}\ \Psi_{elec} \qquad (11)$$

And total energy E_{tot} is sum of E_{elec} and the constant nuclear repulsion energy $E_{nuc} = \sum_{A=1}^{M} \sum_{B>A}^{M} \frac{Z_A Z_{AB}}{R_{AB}}$, which given as [33].

$$E_{tot} = E_{elec} + E_{nuc} \qquad (12)$$

Born–Oppenheimer approximation illustrates the potential energy surface concept (PES). The PES here is determined by E_{elec} (electronic energy eigenvalue invocation by Born–Oppenheimer approximation for electronic Schrodinger equation) of total possible coordinates of the nucleus [29].

Born–Oppenheimer approximation improves our knowledge of the equilibrium geometry and transition state geometry concepts which are sensitive points on the potential energy surface concept PES [29].

2.3.2 Hartree-Fock Self-Consistent Field Method (HF-SCF)

Most of the difficulties in analyzing and resolving Schrödinger equation are coming from that there is a need to define the energy of one electron while it is present in a field of all other electrons at the same time [16].

The HF-SCF takes into consideration these difficulties as it is computing each electron energy in the average static field of other electrons. First, it guesses the energies of electrons, then computes the energy of each electron in the mean field of these electrons. This recursive routine is repeated until convergence is obtained [16].

There are needs to define correlation energy which is the energy difference detained between Schrödinger equation and Hartree-Fock calculations [16].

The HF-SCF computations are accurate enough to highlight a lot of problems, as it is used and applied in various problems. It clarifies that correlation energy is highly important in defining the system properties [16].

2.4 ELECTRON CORRELATION METHODS

In Hartree-Fock Self-Consistent Field Method, each electron moves under the effect of average influence of others. But this approach does not take into consideration of Coulombic electron-electron repulsion interactions. So the movements of electrons are correlated. This correlation causes further separation of electrons. The methods such as Density Functional Theory (DFT) and Møller–Plesset perturbation theory can treat the incapability of HFSCF method including the correlation of electrons in quantum chemical computations [34].

Density Functional Theory (DFT) will be detailed in the next section as it is the method used in this thesis.

2.4.1 Density Functional Theory (DFT)

2.4.1.1 Introduction

One may be asking, what if things being simpler? For instance, instead of working with the wave function, why can't one work with physical observables for determining energy and some other possible properties of the molecule? This question may not surprise researchers if it is asked before discovering of quantum mechanics because such forms are available in classical mechanics [29].

Furthermore, one can take the advantage of knowing the quantum mechanics and ask, which physical observable can be useful? The study of the Hamiltonian operator would be enough to find the physical observable which permit the Hamiltonian operator construction. The Hamiltonian operator depends on the positions (**r**) and atomic

numbers of the nuclei, but the dependence of the Hamiltonian operator especially on the total number of electrons leads to that the physical observable can be useful to be utilized is the electron density (ρ) [29].

2.4.1.2 Electron density

In a given state of electronic system, the number of electrons per unit volume is the electron density $\rho(\mathbf{r})$ for that state, and its formula in terms of wave function is [32]:

$$\rho(\mathbf{r_1}) = N \int_1 \ldots \int_N |\Psi(X_1, X_2, \ldots, X_N)|^2 ds_1 dx_2 \ldots dx_N \quad (13)$$

Integration of this non-negative simple function gives the total number of electrons (N) [32].

$$N = \int \rho(\mathbf{r}) d\mathbf{r} \quad (14)$$

The nuclei's positions correspond to local maxima in the electron density. So atomic number can totally define the Hamiltonian. This information is available from the density because each nucleus (A) located at an electron density maximum ($\mathbf{r}_A$).

$$\left.\frac{\partial \bar{\rho}(r_A)}{\partial r_A}\right|_{r_A=0} = -2Z_A \rho(\mathbf{r}_A) \quad (15)$$

Z_A is the atomic number of A, r_A radial distance from A and $\bar{\rho}$ is spherically averaged density.

The density functional theory of electronic structure is trying to allow the replacement of the complicated N-electron wave function $\Psi\ (X_1, X_2, \ldots, X_N)$ and it's associated Schrodinger equation, by simpler electron density $\rho(\mathbf{r})$ and it's associated calculations. The DFT method's main target is to design functionals which connect the electron density and the energy [32, 33]. Electronic energy of the ground state can be totally defined by electron density (ρ) [31].

Hohenberg and Kohn [35] provided the fundamental two crucial theorems establishing the DFT as a logical quantum chemical methodology [29].

2.4.1.3 First Hohenberg-Kohn Theorem: proof of existence

Hohenberg and Kohn [35] states that, for *N*-electron system, the external potential (V_{ext}) completely fixes the Hamiltonian, thus all properties of the ground state density $\rho(\mathbf{r})$, determined by the *N* and (V_{ext}) [32].

Now, $\rho(\mathbf{r})$ determines the Hamiltonian operator. Also integration of the density gives the number of electrons, so what remaining is defining the operator which determines the external potential, i.e., charges and positions of the nuclei [29].

To proof that ρ determines V_{ext}, assume that two different external potential (V_a) and (V_b) can consistent with same ground state density (ρ_0) [29].

H_a and H_b are belong to two different ground state wave functions, Ψ_a and Ψ_b, and they correspond with E_{0a} and E_{0b}, respectively, noted that $E_{0a} \neq E_{0b}$. Both H_a and H_b only differ in the V_{ext}, then $H_a = T + V_{ee} + V_a$ and $H_b = T + V_{ee} + V_b$ [33].

V_a and V_b appear with two different Hamiltonian operators (H_a) and (H_b), each Hamiltonian associate with ground state Ψ_0, which associated with ground state E_0. H_a expected value over the Ψ_b, should be higher than E_a. That's expressed as below [29]:

$$E_{0a} < \langle \Psi_{0b} | H_a | \Psi_{0b} \rangle \qquad (16)$$

This expression rewritten as:

$$E_{0a} < \langle \Psi_{0b} | H_a - H_b + H_b | \Psi_{0b} \rangle$$

$$< \langle \Psi_{0b} | H_a - H_b | \Psi_{0b} \rangle + \langle \Psi_{0b} | H_b | \Psi_{0b} \rangle$$

$$< \langle \Psi_{0b} | \mathrm{V_a} - \mathrm{V_b} | \Psi_{0b} \rangle + \mathrm{E_{0b}} \qquad (17)$$

Since V is one-electron operators, the integral of last line in Eq. (17) can be written in terms of the ground-state density as:

$$E_{0a} < \int (\mathrm{V_a}(\mathbf{r}) - \mathrm{V_b}(\mathbf{r}))\, \rho_0(\mathbf{r}) d\mathbf{r} + \mathrm{E_{0b}} \qquad (18)$$

As there is no difference between a and b, Eq. (18) can be:

$$E_{0b} < \int (\mathrm{V_b}(\mathbf{r}) - \mathrm{V_a}(\mathbf{r}))\, \rho_0(\mathbf{r}) d\mathbf{r} + \mathrm{E_{0a}} \qquad (19)$$

Now, if we add inequalities (18) and (19), we have:

$$E_{0a} + E_{0b} < \int (\mathrm{V_b}(\mathbf{r}) - \mathrm{V_a}(\mathbf{r}))\, \rho_0(\mathbf{r}) d\mathbf{r} + \int (\mathrm{V_a}(\mathbf{r}) - \mathrm{V_b}(\mathbf{r}))\, \rho_0(\mathbf{r}) d\mathbf{r} + E_{0b} + \mathrm{E_{0a}}$$

$$< \int (\mathrm{V_b}(\mathbf{r}) - \mathrm{V_a}(\mathbf{r}) + \mathrm{V_a}(\mathbf{r}) - \mathrm{V_b}(\mathbf{r}))\rho_0(\mathbf{r}) d\mathbf{r} + E_{0b} + \mathrm{E_{0a}}$$

$$< E_{0b} + \mathrm{E_{0a}} \qquad (20)$$

That means, it's arriving to the next contradiction [33]:

$$E_{0a} + \mathrm{E_{0b}} < E_{0b} + \mathrm{E_{0a}}\ or\ 0 < 0 \qquad (21)$$

This proofs that there cannot be two V_{ext} yields same density, or one can say that the ground state density uniquely specifies the V_{ext}. Recalling eq. (4), then adding the ρ_0 which contains information about $\{N, Z_A, R_A\}$, after summarize, one can get the form of $\rho_0 \Rightarrow \{N, Z_A, R_A\} \Rightarrow \mathrm{H} \Rightarrow \Psi_0 \Rightarrow E_0$ (and all other properties). As the complete ground state energy is a functional of ground state electron density, *Ne* specifies the V_{ext} which defined by the attraction of the nuclei [33].

$$E_0(\rho_0) = T(\rho_0) + E_{ee}(\rho_0) + E_{Ne}(\rho_0) \qquad (22)$$

Now, potential energy due to the nuclei-electron attraction of the system and universal form of N, R_A and Z_A is:

$$E_0(\rho_0) = \int \rho_0(\vec{r}) V_{Ne}\, d\vec{r} + T(\rho_0) + E_{ee}(\rho_0) \qquad (23)$$

where $\rho_0(\vec{r}) V_{Ne}\, d\vec{r}$ represents system dependent part and $T(\rho_0) + E_{ee}(\rho_0)$ represents universally valid part [33].

Combining the system independent parts into a Hohenberg-Kohn functional $F_{HK}(\rho_0)$:

$$E_0(\rho_0) = \int \rho_0(\vec{r}) V_{Ne}\, d\vec{r} + F_{HK}(\rho_0) \qquad (24)$$

The functional $F_{HK}(\rho_0)$ at first sight, looks like the desired formula of DFT, If we could know it exactly, then we could reach the exact solution of the Schrodinger equation. And because it is a system independent, we could get exact solutions for the systems from hydrogen atom to DNA. But unfortunately, it is not possible to know the exact forms of the $T(\rho_0)$ and the $E_{ee}(\rho_0)$ [33].

Up to here, one can say that ground state density is principally enough to obtain all system properties. But how to make sure that a defined density is desired ground state density? [33]

2.4.1.4 Second Hohenberg-Kohn Theorem: variational principle

The Second Hohenberg-Kohn theorem states that the functional $F_{HK}(\rho_0)$ drives to the system energy at the ground state, also drives to minimum energy only if the density is real ground state density ρ_0 [33]. According to the variational principle, this can be expressed as:

$$E_0 \leq E(\tilde{\rho}) = T(\tilde{\rho}) + E_{Ne}(\tilde{\rho}) + E_{ee}(\tilde{\rho}) \qquad (25)$$

Any trial density $\tilde{\rho}(\mathbf{r})$ defines its own H and its own $\widetilde{\Psi}$. This wave function can now be taken as the Ψ_{trial} for the H generated from the true $V_{ext.}$. Next equation will lead to the desired result [33].

$$\langle \widetilde{\Psi} | \tilde{H} | \widetilde{\Psi} \rangle = T(\tilde{\rho})\, V_{ee}(\tilde{\rho}) + \int \tilde{\rho}(\vec{\mathbf{r}}) V_{ext}\, \mathrm{d}\vec{\mathbf{r}} = E(\tilde{\rho}) \geq E_0(\rho_0) = \langle \Psi_0 | H | \Psi_0 \rangle \quad (26)$$

2.4.1.5 The Kohn-Sham approach

To put the HK theorems into reality, and construct its calculations, Kohn and Sham (KS) [36], used HF theory in introducing an imaginary system of *N* non-interacting electrons which have the same density as real system. The ground state wave function Ψ_0 of this system expressed by a single Slater determinant. Kohn–Sham orbital (ϕKS) forms this Slater determinant which is the solutions of *N* single particle equations. According to the variational principle, the variations in ϕKS determines ground state energy and the ground state density [37].

Where the (KS) one-electron operator is defined as [29]:

$$h_i^{KS} = -\frac{1}{2}\nabla_i^2 - \sum_k^{nuclei} \frac{Z_k}{|r_i - r_k|} + \int \frac{\rho(r')}{|r_i - r'|} dr' + V_{xc} \qquad (27)$$

and

$$V_{xc} = \frac{\delta E_{xc}}{\delta \rho} \qquad (28)$$

V_{xc} is one-electron operator, and E_{xc} is the V_{xc} expectation value for the KS Slater determinant.

Contribution of KS-energy essentially comes from the exchange correlation energy (E_{XC}). The E_{XC} contains corrections of kinetic energy due to the electron-electron repulsions, and interaction correlations in a system need to be corrected [37].

2.5 BASIS SETS

The basis set is a set of mathematical functions which used to construct the wave function [29].

The electronic structure computations over molecules propose that the molecular wave function expressed in linear Combination of Atomic Orbitals (LCAO), The AO functions can be assumed to solve Schrödinger equation for the hydrogen atom [34].

LCAOs are used to define molecular orbitals (MOs). Each MO is a single electron wave function, and *N* electron of MO combined to form *N* electron wave function. The system with more than one electron cannot be described by the molecular orbitals or even by the atomic orbitals. To describe such a system, one needs *N*-body wave functions. MOs are utilized to construct good approximations of the *N* electron wave function [38].

For solving the electronic Schrödinger equation of a molecule, each one-electron functions considered as molecular orbital, which are produced from spatial orbital and spin function (α, β) [31].

There are a lot of approximation methods for solving Schrödinger equation and utilizing of one of these methods for solving a specific problem usually done by comparing its performance with a known experimental data. Thus, letting the experimental data drive the selection of choosing the method of the computational model is better than preceding the computational procedure directly [31].

Introducing the basis set is one of the approximations basically exists in *ab initio* methods. If the basis set is complete, the expanding of known function as MO in another known function is not an approximation, because a complete basis set has to use an infinite number of functions, which considered impossible in actual calculations [31].

The expanding of MOs drives to the integration of QM operators over basis function, and the ease of calculating these integrals depends on the type of basis function [31].

2.5.1 Slater and Gaussian Type Orbitals basis set (STO/GTO)

The *ab initio* MO calculations need to be simplified enough to be applied in relatively large molecules. One of the widely used methods is a linear combination of atomic orbitals self-consistent field (LCAO-SCF). This LCAO-SCF uses a minimal basis set of STO's [39].

The wave functions of hydrogen have the form: $\psi nlm(\mathrm{r},\theta,\varphi) = \mathrm{R}nl(\mathrm{r})\mathrm{Y}ml(\theta,\varphi)$. The radial part, $\mathrm{R}nl(\mathrm{r})$, of this hydrogen wave function is a polynomial in r, which is the distance from the origin. This polynomial is a simplification, and drives to Slater Type Orbitals (STO), and given as [38]:

$$\varphi_{STO}(\mathrm{r}_A,\theta,\varphi;\ n,m,l,\zeta) \ = \ N\mathrm{r}_A^{n-1}\exp(-\zeta\ \mathrm{r}_A)\ Y_{ml}(\theta,\varphi) \qquad (29)$$

N is normalization constant, spherical coordinate system (r_A,θ,φ) is defined around atom *A*, and parameter Zeta (ζ) is the orbital exponent.

Full STO calculations are consuming a large time because of the two electron integral evaluation. Since the integrals of Gaussian functions can be analytically evaluated, so it is possible to replace each STO by a linear combination of small number of GTOs [39].

The GTOs replaces $\exp(-\zeta\ \mathrm{r})$ with $\exp(-\alpha\ r^2)$, giving spherical Gaussians the form of [38]:

$$\varphi_{sGTO}(\mathrm{r},\theta,\varphi;\ n,m,l,\alpha) \ = \ N\mathrm{r}_A^{n-1}\exp(-\alpha\ \mathrm{r}^2)\ Y_{ml}(\theta,\varphi) \qquad (30)$$

Cartesian Gaussians have the form:

$$\varphi_{GTO}(r;\ i,j,k,\alpha) \ = \ N\ X_A^i\ Y_A^j\ Z_A^k\ \exp(-\alpha\ |\mathbf{R}A\ -\ r|^2) \qquad (31)$$

N is the normalization constant, the coordinate $\mathbf{R}_A = (X_A,Y_A,Z_A)$ defines the center of the GTO, r = (x,y,z) expresses the Cartesian coordinate and GTO is being evaluated. The sum of the integers *i*, *j*, and *k* indicates the angular momentum of the GTO [38].

And, $L = i + j + k$ (32)

By comparing between STO and GTO, the STO has correct cusps as distance decreases from the center to zero, and decays similar to hydrogen as distance increases. GTOs have incorrect behavior at decreased *r*, and rapidly decay at increased *r*. But,

GTOs are more introduced for practical considerations, because their mathematical properties allow faster evaluations of the integrals. [38].

The incorrect cusp and long range decay of the GTO can be fixed by using a linear combination of Gaussian functions each with a unique orbital exponent to form a contracted Gaussian basis function (CGTO) [38].

$$\varphi_{CGTO}(r) = \sum_k d_k \, \varphi_{GTO}(r; \alpha_k) \qquad (33)$$

2.5.2 Minimal basis set

In this basis, there is one function STO, CGTO, or GTO used for AO. The general representative of this basis is STO-nG, e.g. in the STO-3G basis set, there are three primitive GTO combined into one CGTO [33].

This nomenclature means that each type of orbital core through valence defined by only one basis function. Thus for H and He, they have only 1s function, Li to Ne have five functions, i.e, *1s*, *2s*, *2px, 2py*, and *2pz*. For Na to Ar, there are four functions *3s, 3px*, *3py*, and *3pz* which added to the five of second-row making total functions nine functions, etc [29].

2.5.3 Split-Valence (Pople) basis sets

In the STO-3G basis set, one can construct two basis functions for each AO. This won't double the size of basis set, but the size of equation will be increased. Consequently, this will double ζ. This kind of basis set with two functions for each AO is called a 'double-ζ ' basis [29].

The changes in electronic wave function happens in the valence space. If one can limit the doubling of set of functions in the valence orbitals, while keeping the inert core electrons in minimal set, this will define the split-valence type set [33].

Pople and coworkers [40, 41], developed split-valence basis sets, the typical notation for Pople basis sets is X-YZg. X indicates the Gaussians primitive number used in inert core functions. The Y and Z represent valence orbitals primitives, if there are two basis functions then it is double-ζ basis, if it is composed of three functions, then it is valence of triple-ζ, etc [29].

In Pople basis set notation, * indicates polarization functions for all atoms except hydrogen, and ** denotes that all atoms have polarization functions including hydrogen. If the notation contains +, it means there are diffuse functions for all atoms except hydrogen, and ++ shows that hydrogen has diffusion functions too [38].

In next two tables, 2.1 showing some examples of Pople style basis sets and their composition according contracted and primitive basis functions, and 2.2 showing the designation of the 6-31g(d) basis set.

Table 2.1 Composition of basis sets in terms of contracted and primitive basis functions for some Pople style basis sets [31].

Basis	Hydrogen		First row elements		Secondrow elements	
	Contracted	Primitive	Contracted	Primitive	Contracted	Primitive
STO-3G	*1s*	*3s*	*2s1p*	*6s3p*	*3s2p*	*9s6p*
3-21G	*2s*	*3s*	*3s2p*	*6s3p*	*4s3p*	*9s6p*
6-31G(d,p)	*2s1p*	*4s*	*3s2p1d*	*10s4p*	*4s3p1d*	*16s10p*
6-311G(2df,2pd)	*3s2p1d*	*5s*	*4s3p2d1f*	*11s5p*	*6s4p2d1f*a	*13s9p*a*

*McLean–Chandler basis set [42]

Table 2.2 6-31g(d) designation [31].

6-31g(d)	6 primitive gaussian type orbitals GTOs
-	Split valence
31	Atomic orbitals
G	Gaussian type orbitals
(d)	d- type orbitals for heavy atoms

2.5.4 Correlation-Consistent basis sets

Dunning [43], designed the correlation consistent polarized valence for optimizing correlated methods (Post-Hartree–Fock methods) using extrapolation techniques. The polarization function is included in this basis set, and it is abbreviated as cc-pVxZ, where VxZ denotes the functions number used for each valence AO, and x is zeta basis which is D= double, T= triple, etc. [38].

Dunning [43] studied correlation effects in the oxygen atom and established that the Primitive Gaussian functions describe correlation when exponents of functions optimized in atomic correlated calculations. These calculations on oxygen atom work as guidance for the atoms of first row from B to Ne. The *spdfg* sets used for correlated molecular calculations were defined for all these atoms.

Concept of correlation consistent basis sets states that, due to the addition of correlation functions, the incremental energy decreases in distinct groups. Thus *1s1p* set and *1d* function decrease the correlation energy, also incremental energy decrease for *2s2p*, *2d* and *1f* sets are similar. For the first row atoms, *sp* set is shown in table 2.3 [43].

Table 2.3 The *sp* set [43].

	Primitive	Contracted	Polarization set
cc-pVDZ	*(9s4p)*	*(3s2p)*	(1d)
cc-pVTZ	*(10s5p)*	*(4s3p)*	(2d 11)
cc-pVQZ	*(12s6p)*	*(5s4p)*	(3d2/1g)

2.5.5 Exchange-Correlation Functional

The E_{XC} in equation (28) contains the differences in kinetic energy between the imaginary system and real one. The E_{xc} functional and energy density (ε_{XC}) are dependent on electron density [29].

$$E_{XC}\,(\rho(r)) = \int \rho(r)\varepsilon_{XC}\,(\rho(r))dr \qquad (34)$$

2.5.6 B3LYP DFT Method

B3LYP functional, pro-nounced as "B-three-lip", is a linear combination of the Local Density Approximation (LDA), the B88 functional [44], and the LYP functional (Lee, Yang and Parr) [45]. B3LYP method combines Becke's generalized gradient approximations (GGA) exchange with the GGA correlation functional of Lee, Yang, and Parr [38].

In this method, the exchange-correlation energy (E_{xc}) of Kohn-Sham density functional theory is given by this formula [46]:

$$E_{XC} = \int_0^1 U_{XC}^{\lambda} \, d\lambda \qquad (35)$$

Where λ is an interelectronic coupling-strength parameter, $U_{XC}^{\boldsymbol{\lambda}}$ is the potential energy of exchange correlation.

When the λ=0 limit of the coupling-strength integration in Eq. (35) is exact exchange, therefore, exact exchange energy play a role in highly accurate DFTs. Consequently, the following exchange-correlation approximation is proposed [46]:

$$E_{XC} = E_{XC}^{LSDA} + a_0(E_X^{exact} - E_X^{LSDA}) + a_X \Delta E_X^{B88} + a_C \Delta E_C^{PW91} \qquad (36)$$

In equation (36), a_0, a_X, a_C are semi-empirical coefficients to be determined by an appropriate fit to experimental data, (E_X^{exact}) is the exact exchange energy, (ΔE_X^{B88}) is Becke's 1988 gradient correction for exchange and (ΔE_C^{PW91}) is the 1991 gradient correction for correlation of Perdew and Wang [44, 47].

In this thesis, a theoretical investigation conducted using Gaussian09 software [48] and a Density Functional theory methodology, and calculations are performed for the optimization of geometries, frequencies of reactants, transition states and products.Then energetic properties of reaction systems are revealed.

This applied DFT method utilized Becke's three parameter exchange function with Lee-Yang-Parr correlation function (B3LYP) and a basis-set of 6-311G(d).

This methodology is used to investigate the details of the reaction of carbonyl sulfide absorption by aqueous diethanolamine solution.

Claculated thermochemical and reaction kinetics properties are compared with the experimental data avialable in the literature, and the most propable reaction mechanism is revealed.

CHAPTER 3

RESULTS AND DISCUSSION

To investigate the reaction of carbonyl sulfide absorption in aqueous diethanolamine, (COS/DEA/H2O system), modeling of four different reaction mechanisms according to proton transfer from one molecule to another is performed. Then quantum chemical calculations by Gaussian09 are proceeded to get optimized geometries, thermal data, vibrational properties and some other physiochemical properties.

After preceding the Gaussian09 calculations, some thermal and kinetic data extracted from the computational results. These thermal and kinetic data will be compared with experimental ones obtained from the literature.

Reaction components of all these four suggested mechanisms are optimized geometrically at the three states, reactants (R), transition (TS) and products (P). Figure 3.1 shows the steps which are followed in this study.

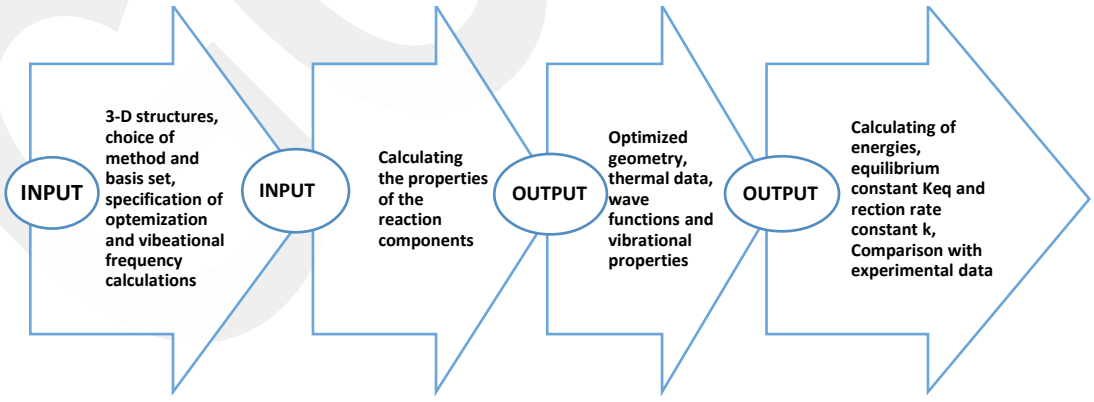

Figure 3.1 Flowchart of study steps followed in this work.

3.1 PROCESSING

The work in this investigation starts with drawing of 3-D structures of carbonyl sulfide, diethanolamine and water, which are the molecules involved in the studied reaction. And then they are used together to prepare the suggested four termolecular reaction mechanisms to be ready for processing the computations.

After preparing the input files and stating the method, the basis set and other input parameters, it is time to ask the Gaussian to start its process of calculating and computing the geometry optimizations, frequencies, structural properties and thermal properties of each file of the four suggested reaction mechanisms.

Each mechanism calculated in three files, one file for each reaction stage, reactants, transition state and products.

This process takes time, depending on the treated molecular structures, number of atoms in the system, size of the atoms and method and basis set used.

The outputs of the computation process will provide us with the optimized geometry, vibrational properties and thermal data.

3.2 GEOMETRY and VIBRATIONAL CALCULATIONS

3.2.1 Geometry Optimizations

Reaction systems following the four different mechanisms are optimized at the B3LYP/6-311G(d) level of theory. Chemical structures of reactants, transition state and products of these optimized reaction systems are given below.

3.2.1.1 DWOCS, DEA (proton of nitrogen)_water_O=C=S.

In this reaction system, the proton attached to the nitrogen atom in diethanolamine transfers to the water molecule, then moves towards oxygen atom attached to carbon of carbonyl sulfide. Figures 3.2 A, B and C represent the reactants, transition state and products of the reaction system, respectively.

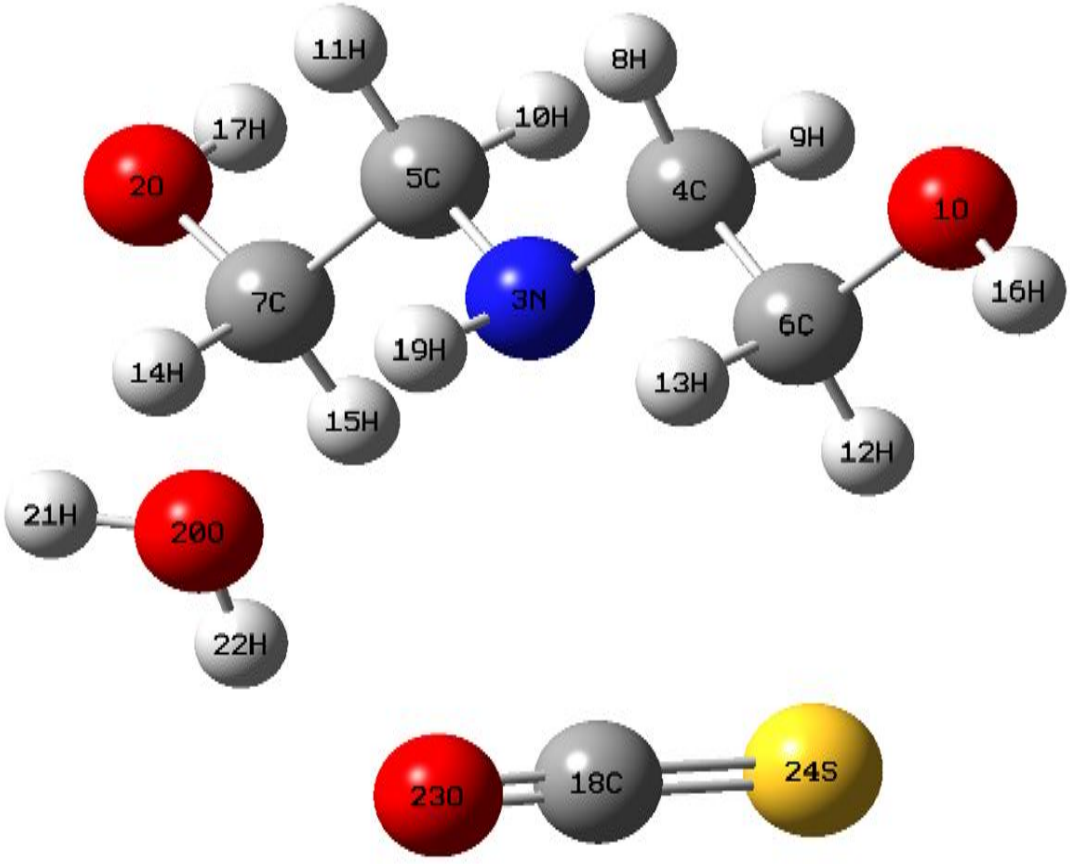

Figure 3.2 A. DWOCS_R reactants

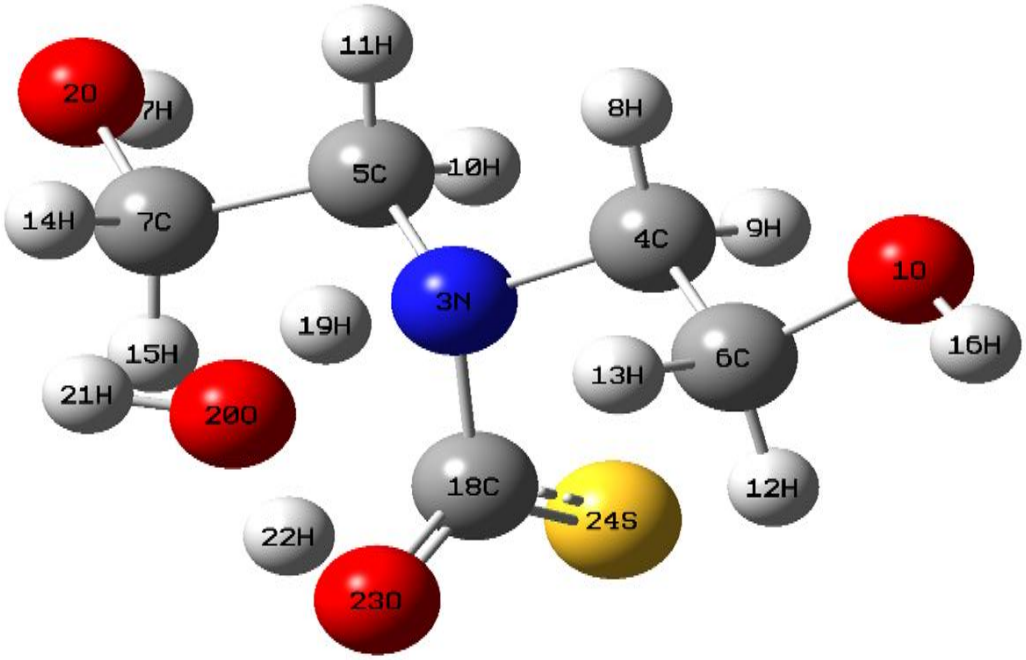

Figure 3.2 B. DWOCS_TS transition state

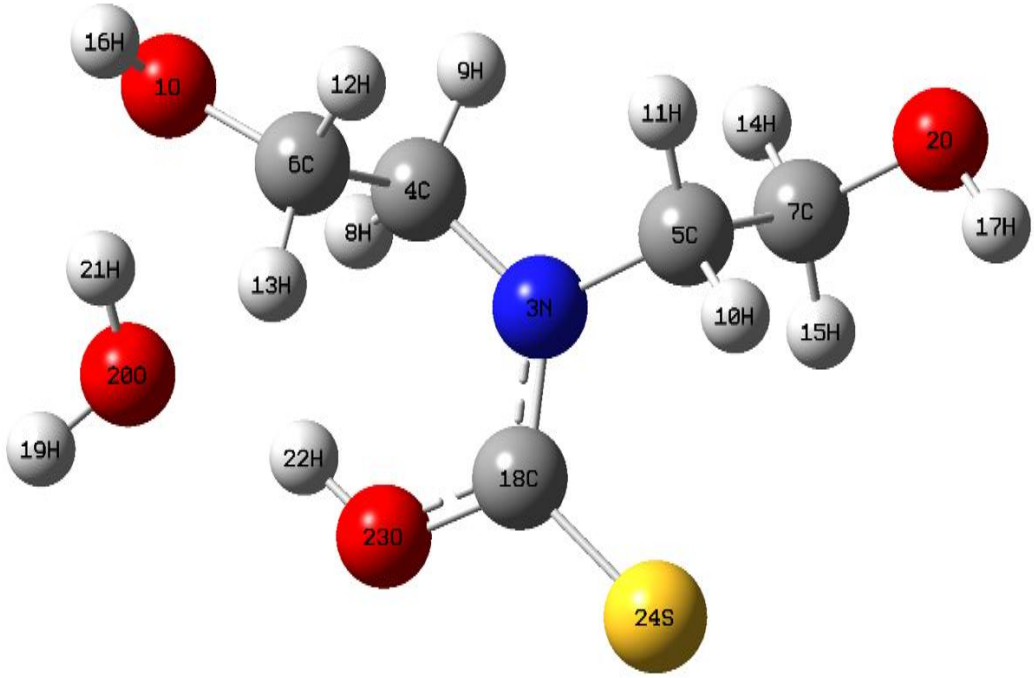

Figure 3.2 C. DWOCS_P products

3.2.1.2 DWSCO, DEA (proton of nitrogen)_water_S=C=O.

In this mechanism, the proton attached to the nitrogen atom in diethanolamine transfers to the water molecule, then moves towards sulfur atom attached to carbon of carbonyl sulfide. Figures 3.3 A, B and C show the reactants, transition state and products of the reaction system, respectively.

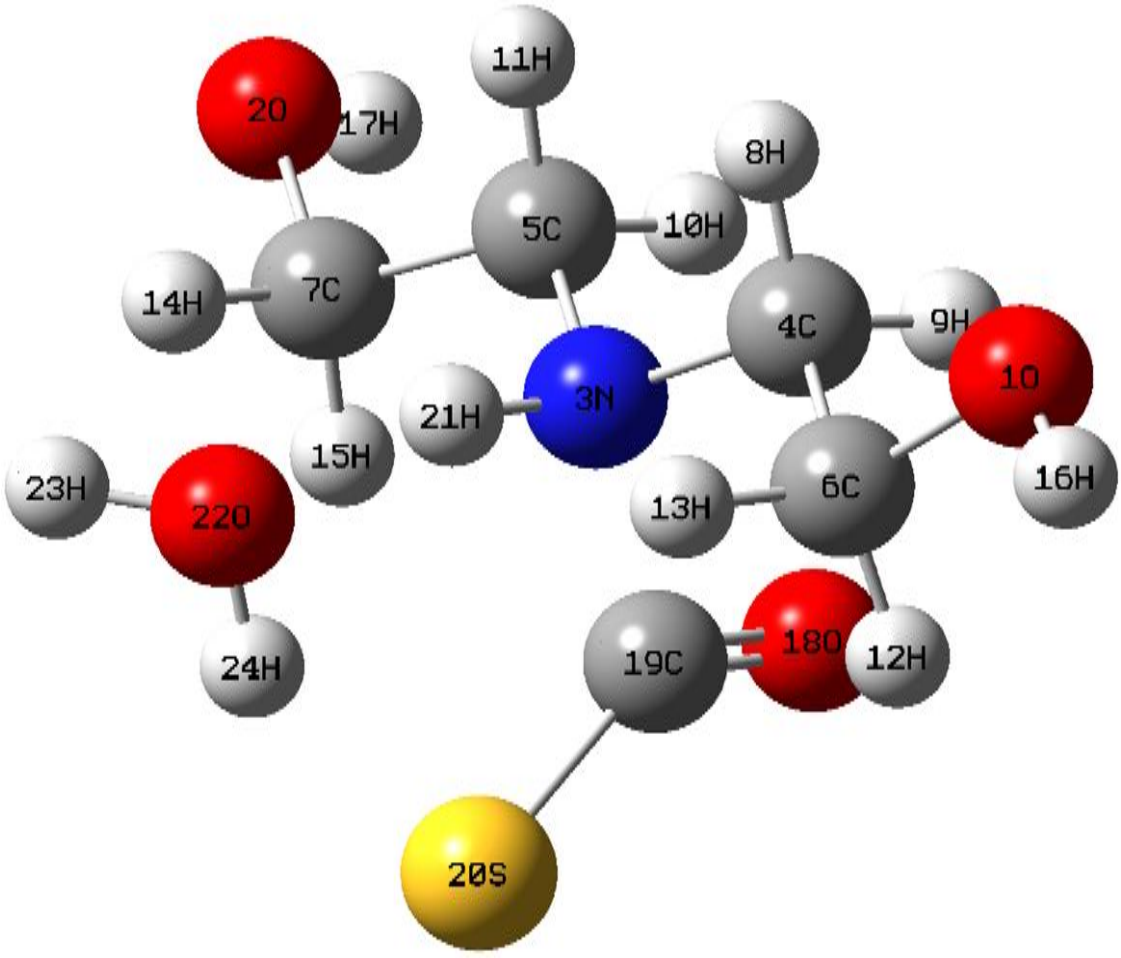

Figure 3.3 A. DWSCO_R reactants

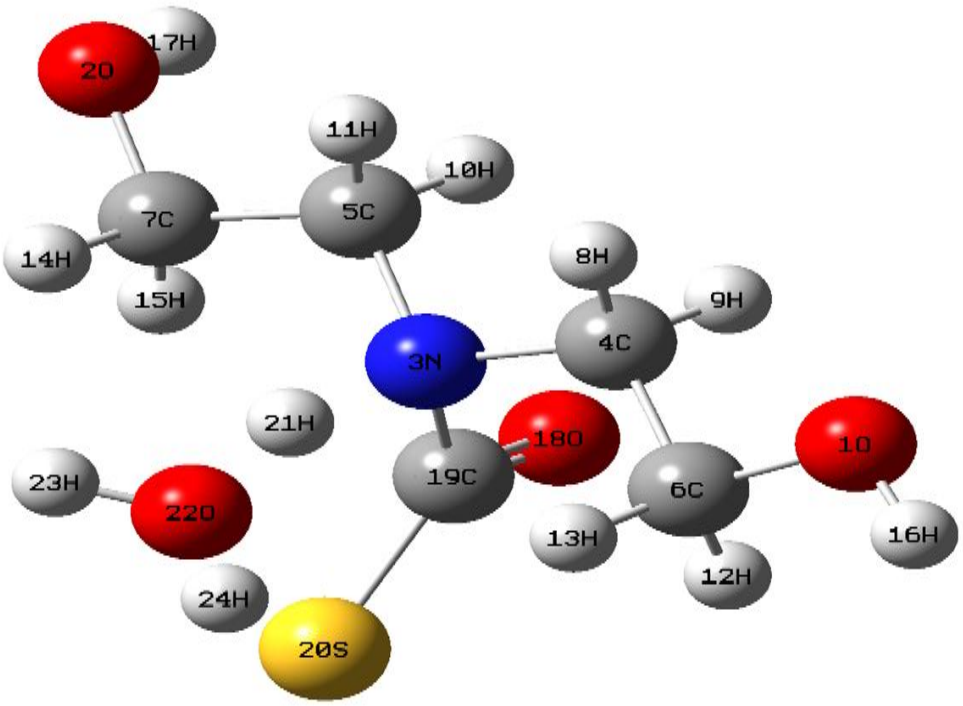

Figure 3.3 B. DWSCO_TS rransition state

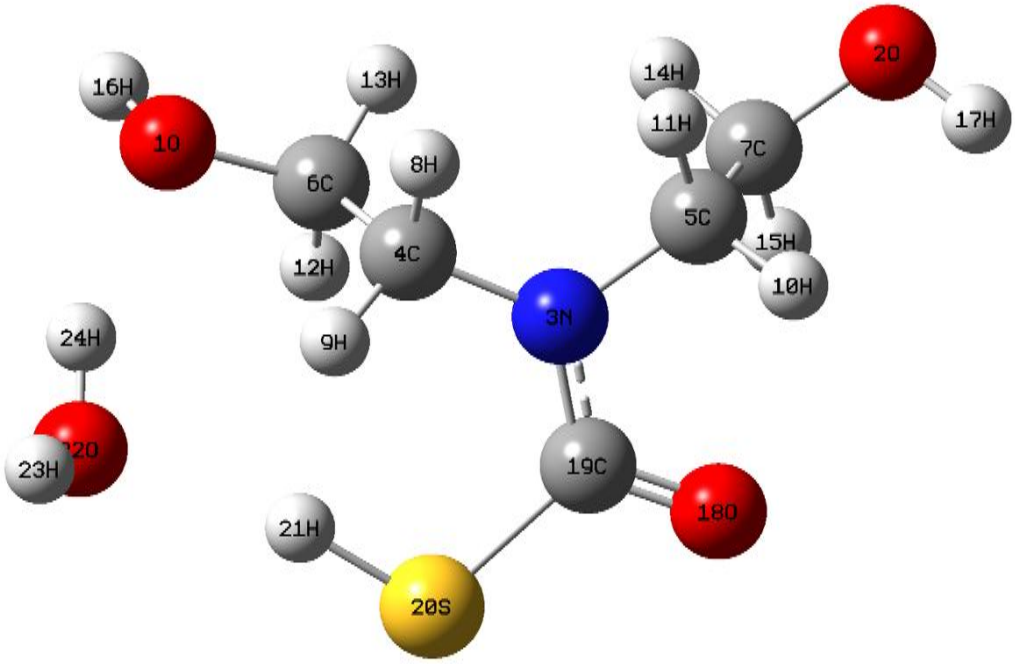

Figure 3.3 C. DWSCO_P products

3.2.1.3 WDOCS DEA (proton of OH in amine)_water_O=C=S.

In this mechanism, the proton of the hydroxyl group in diethanolamine transfers to the water molecule, then moves towards oxygen atom attached to carbon of carbonyl sulfide. Figures 3.4 A, B and C represent the reactants, transition state and products of the reaction system, respectively.

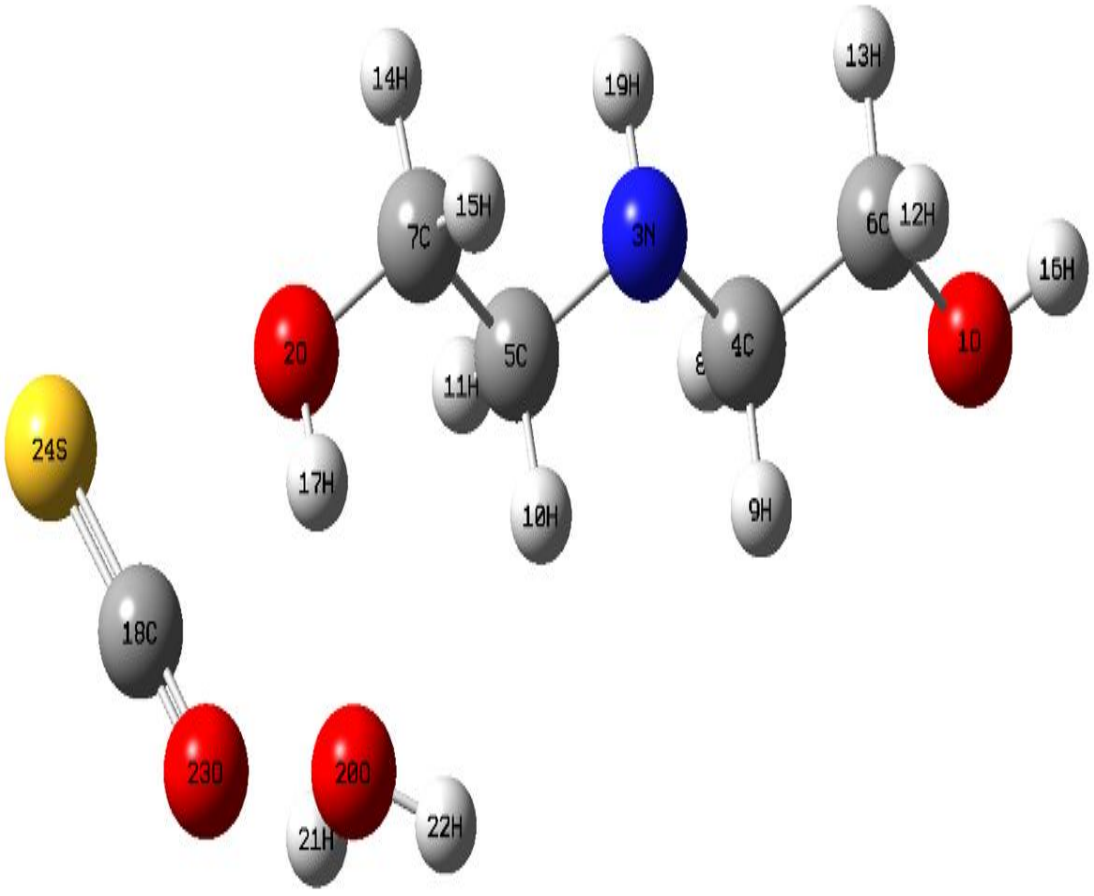

Figure 3.4 A. WDOCS_R reactants

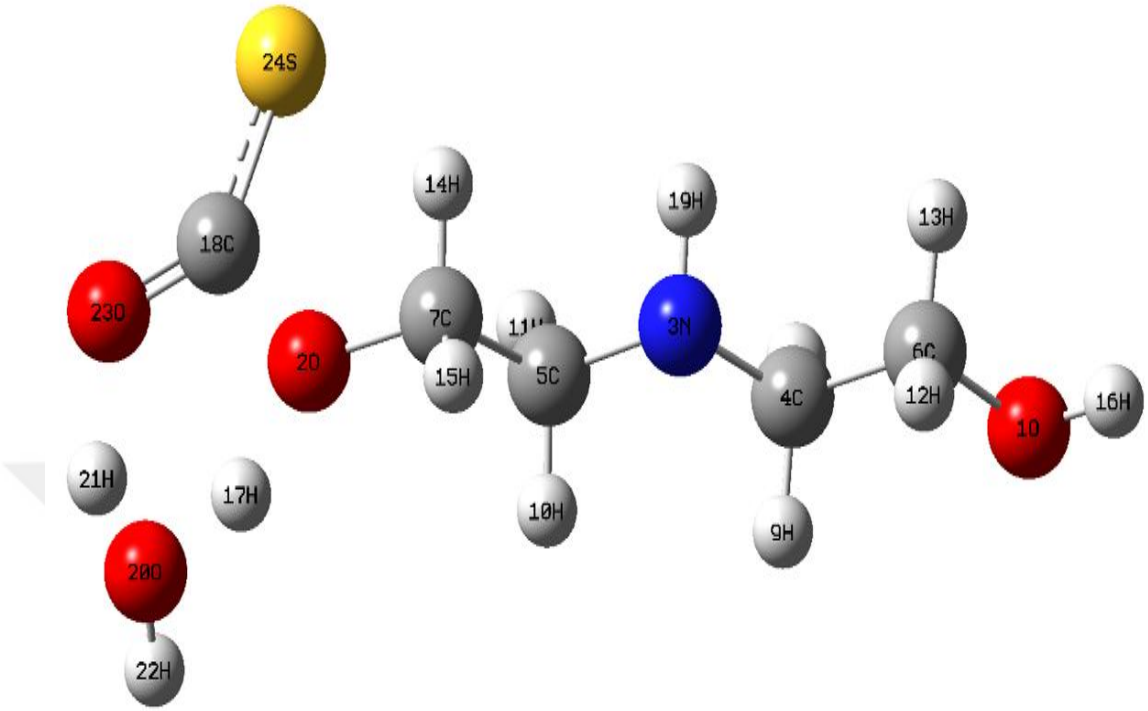

Figur 3.4 B. WDOCS_TS transition state

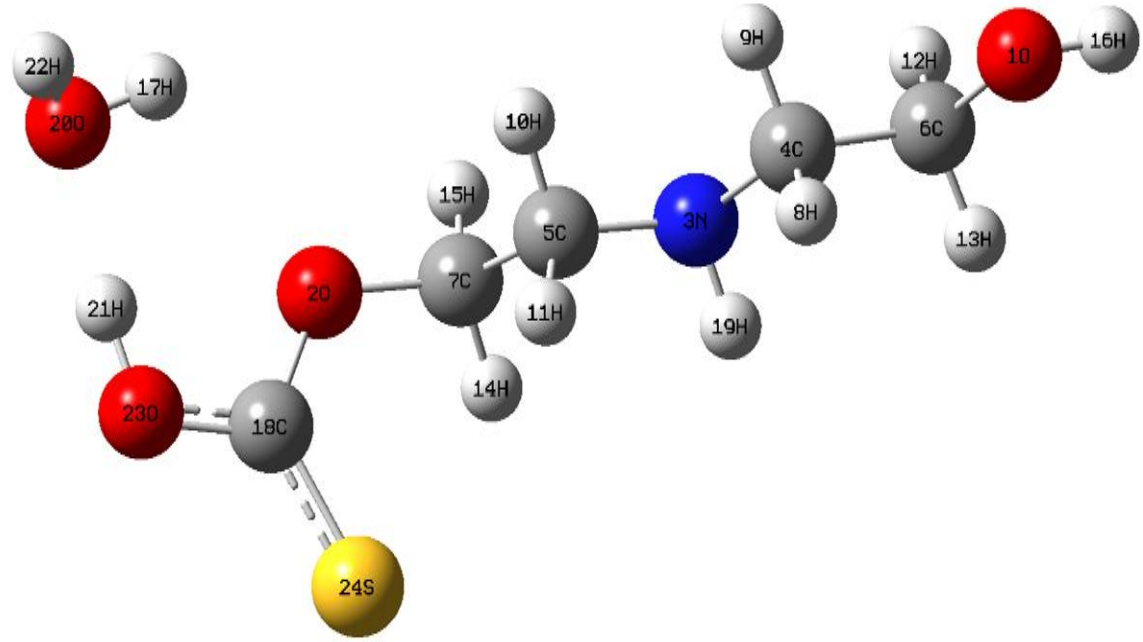

Figure 3.4 C. WDOCS_P products

3.2.1.4 WDSCO DEA (proton of OH in amine)_water_S=C=O.

In this mechanism, the proton of the hydroxyl group in diethanolamine transfers to the base water molecule, then moves towards sulfur atom attached to carbon of carbonyl sulfide. Figures 3.5 A, B and C show the reactants, transition state and products of the reaction system, respectively.

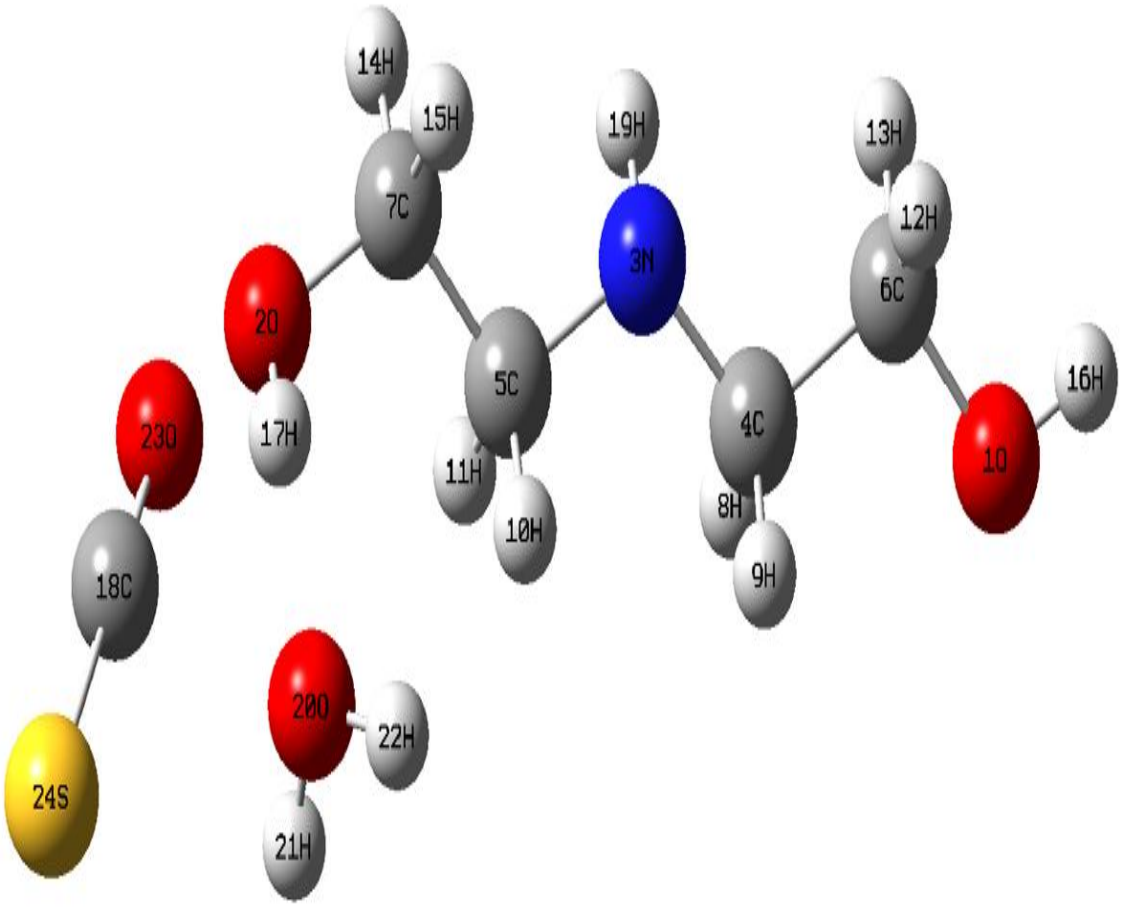

Figur 3.5 A. WDSCO_R reactants

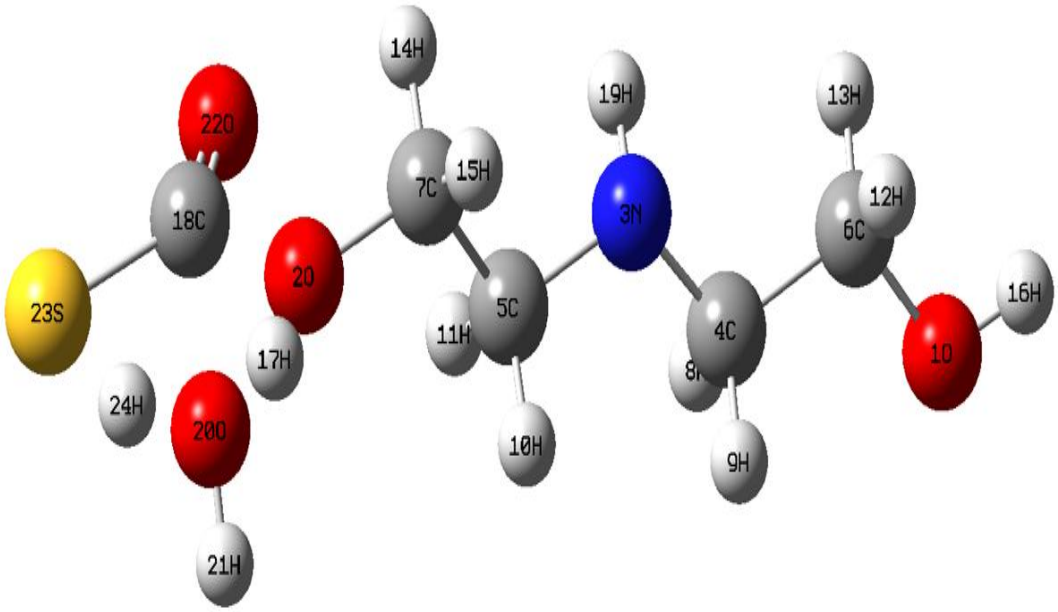

Figur 3.5 B. WDSCO_TS transition state

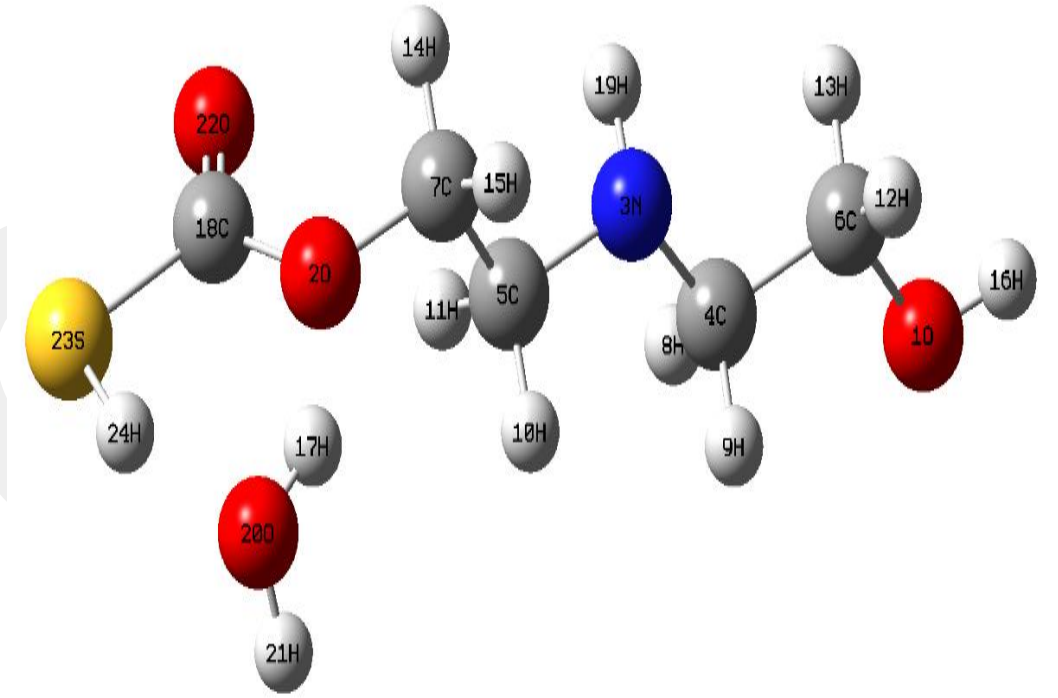

Figur 3.5 C. WDSCO_p Products

3.3 STRUCTURAL PROPERTIES

This section reports bonds lengths, carbonyl sulfide S=C=O or O=C=S angles and dihedral angles for the four reaction mechanisms. Figures 3.6 A-D show the atoms labels, and Tables 3.1 A-D, illustrate the measured values (bond lengths in Å, bond and dihedral angles in ˚).

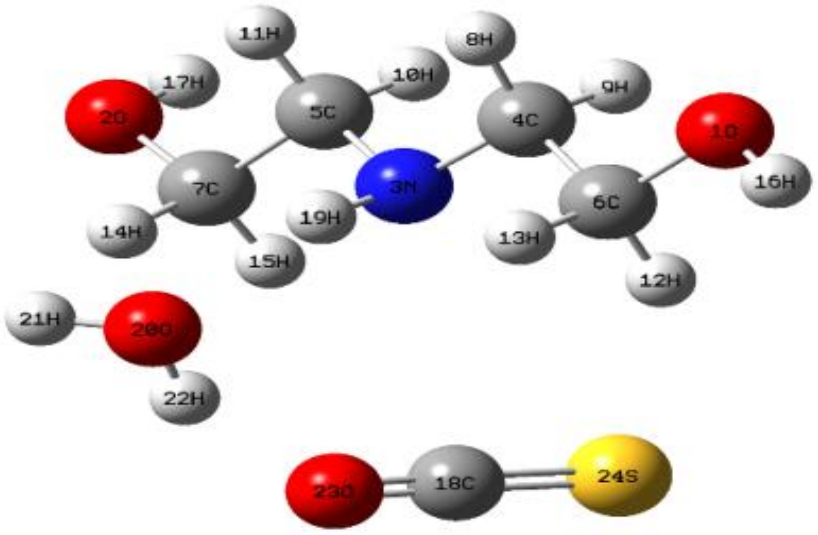

Figure 3.6 A DWOCS R

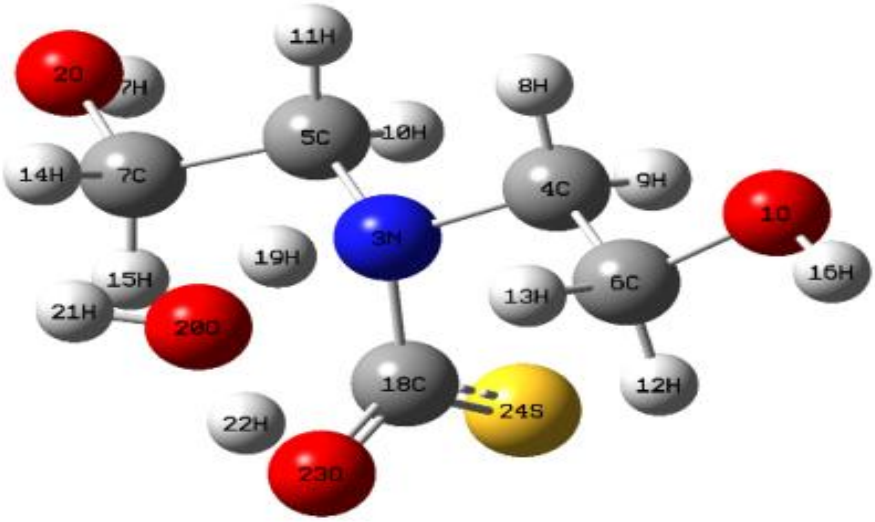

Figure 3.6 A DWOCS Ts

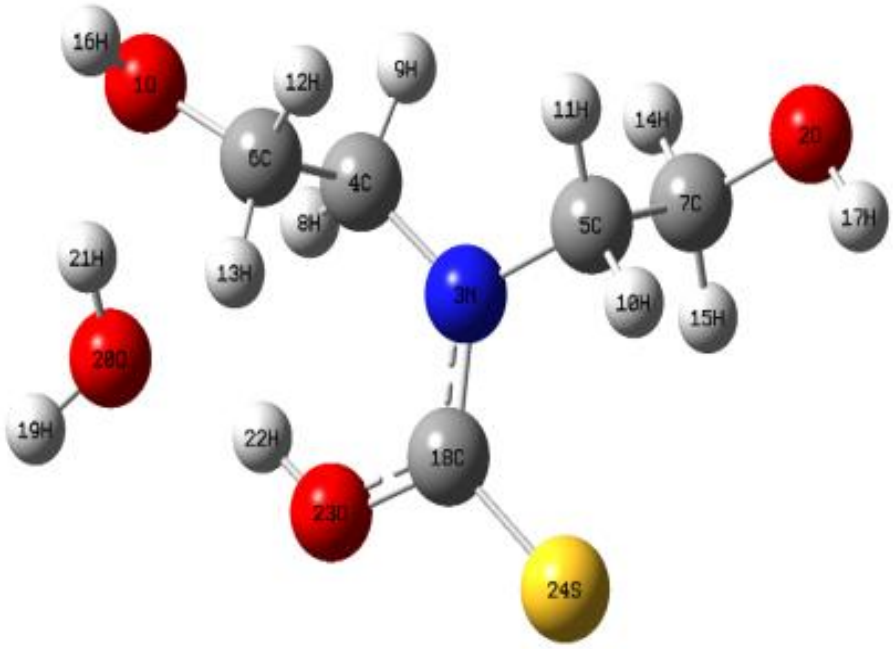

Figure 3.6 A DWOCS P

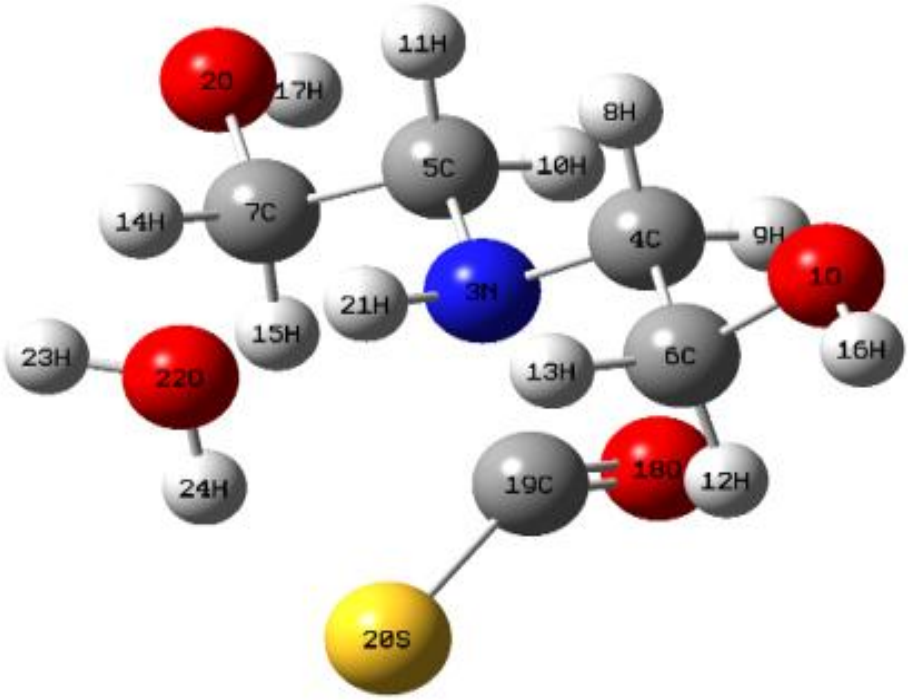

Figure 3.6 B. DWSCO R

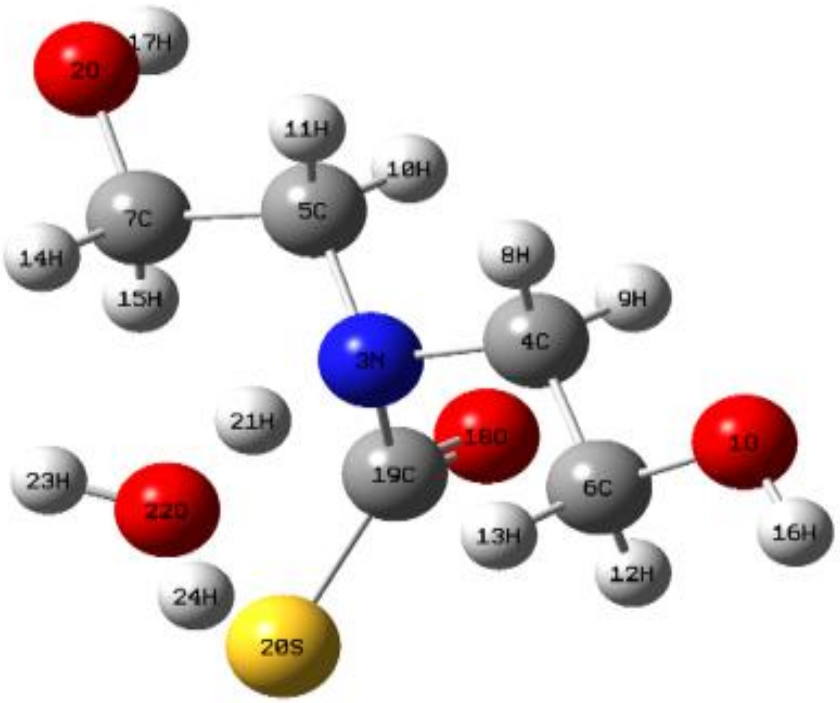

Figure 3.6 B. DWSCO Ts

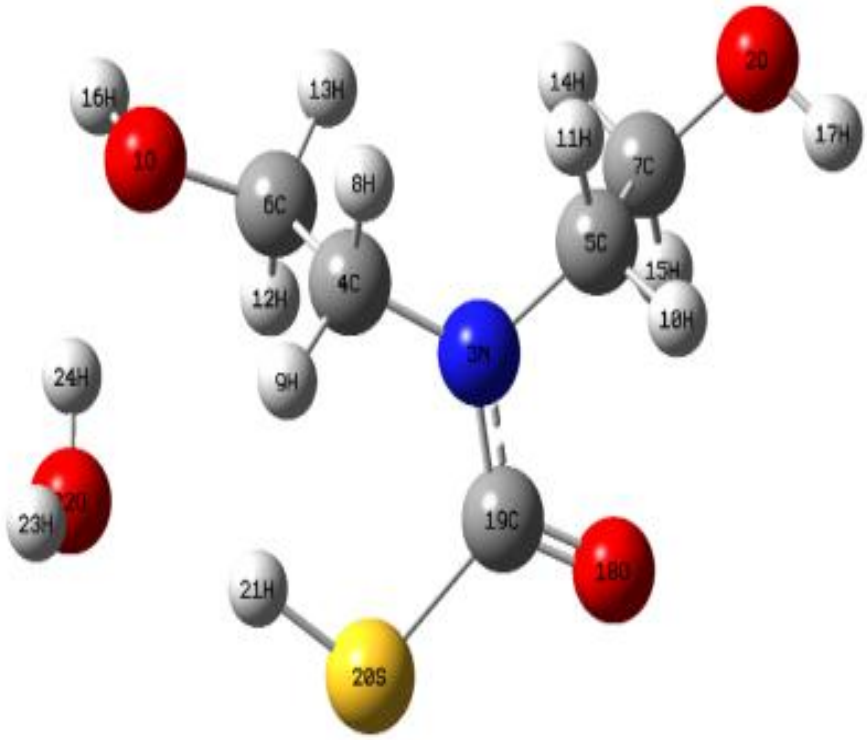

Figure 3.6 B. DWSCO P

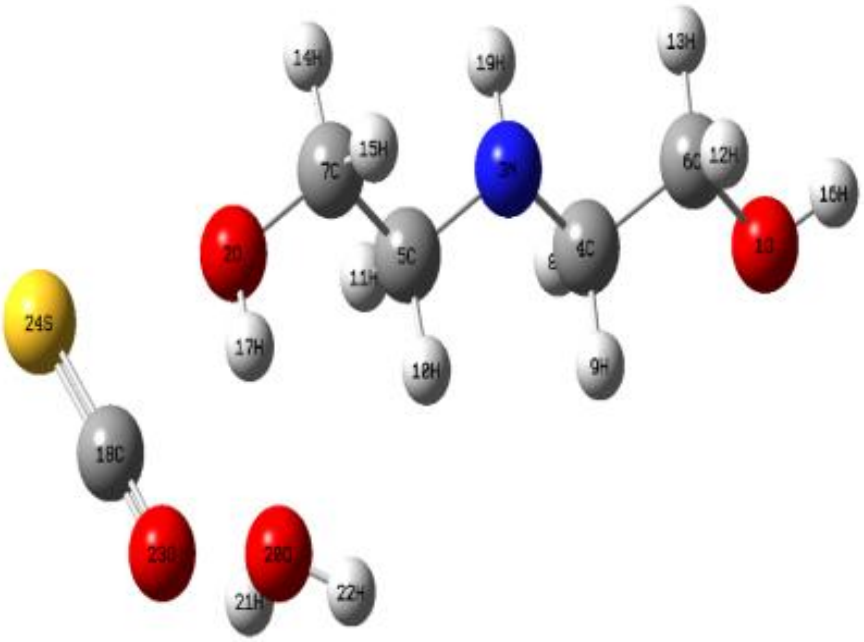

Figure 3.6 C WDOCS R

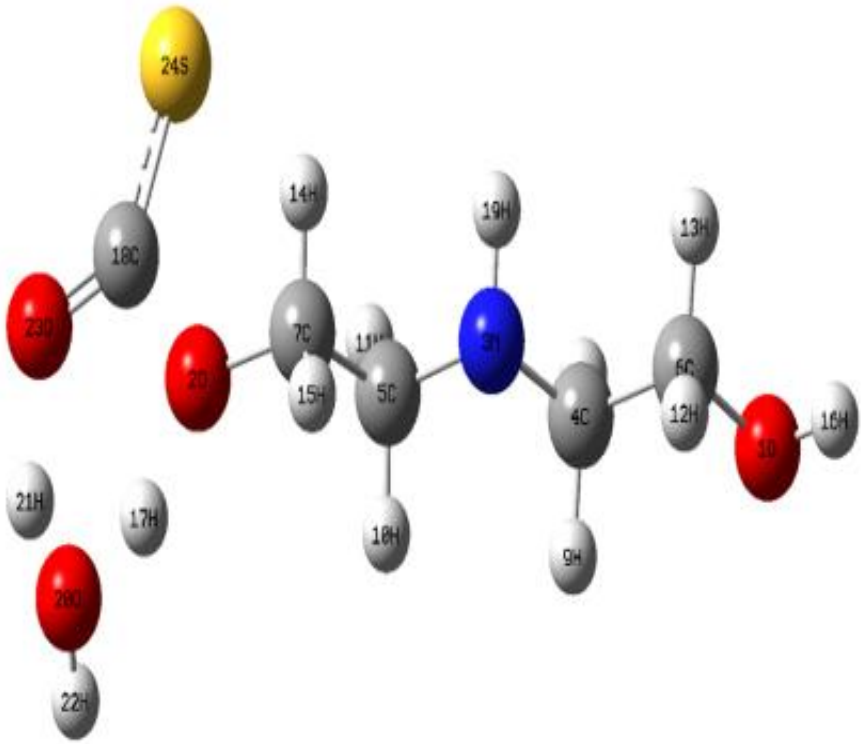

Figure 3.6 C WDOCS Ts

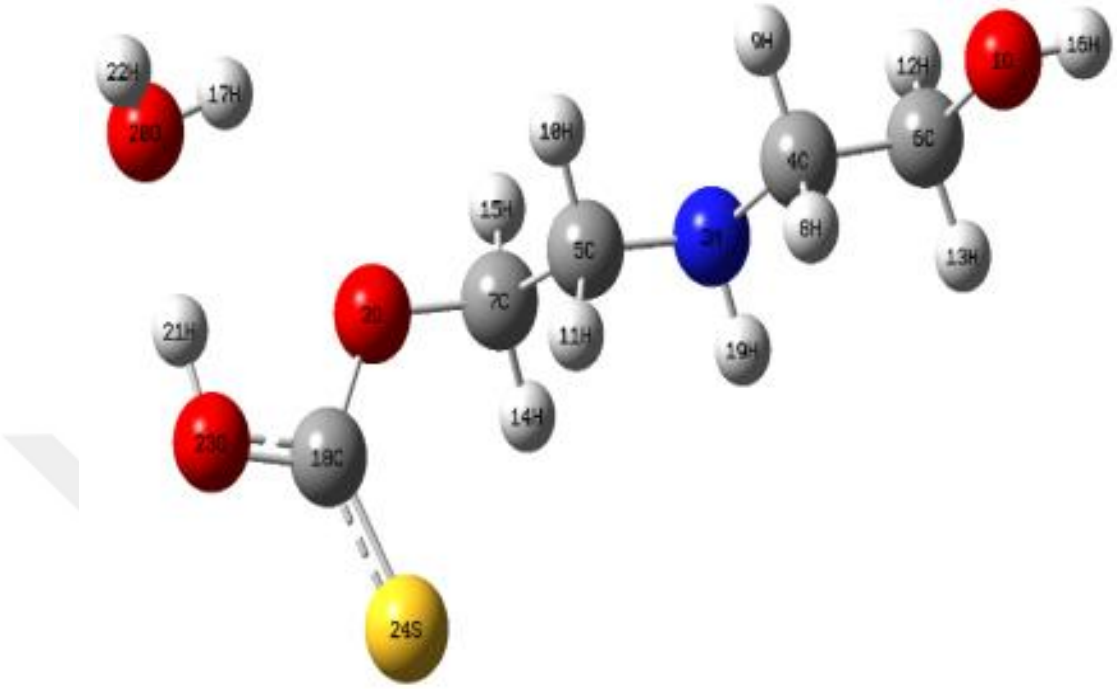

Figure 3.6 C WDOCS P

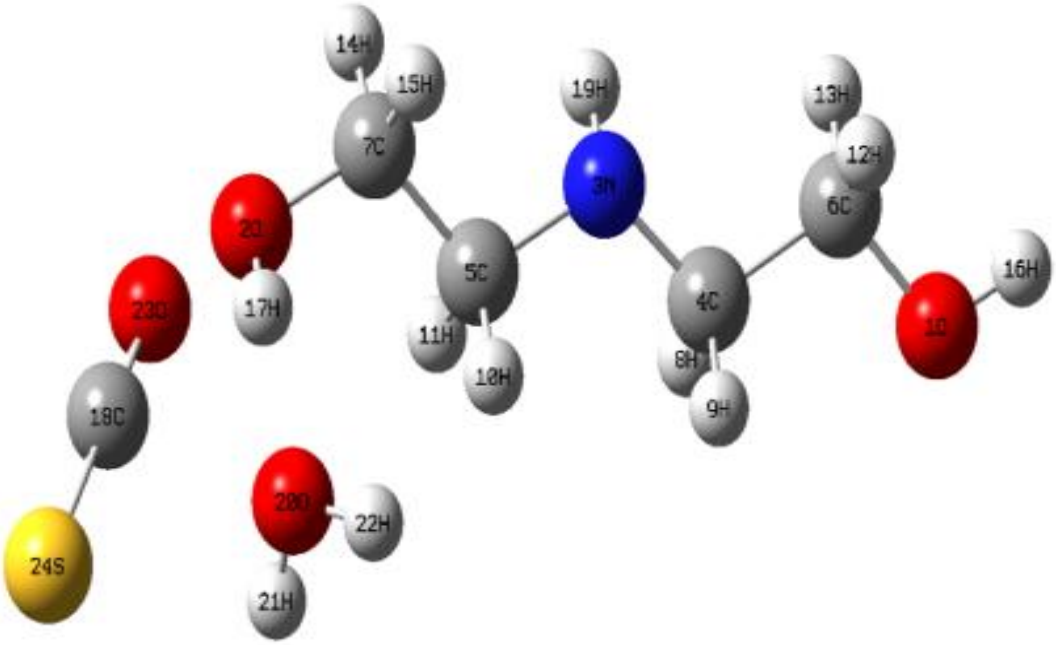

Figur 3.6 D. WDSCO R

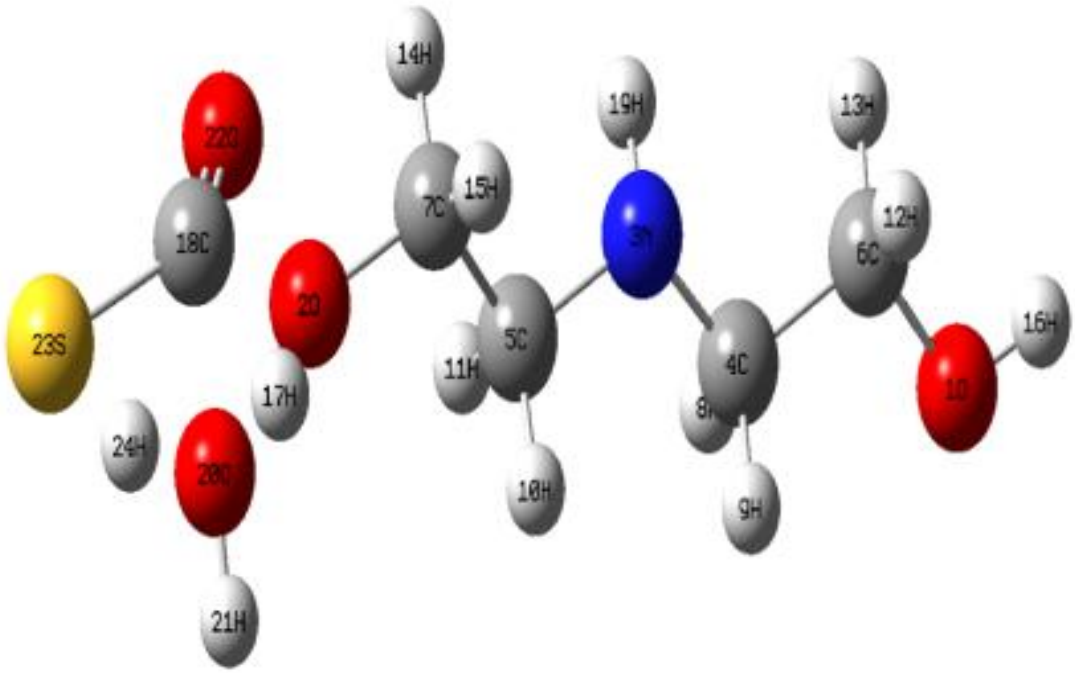

Figur 3.6 D. WDSCO Ts

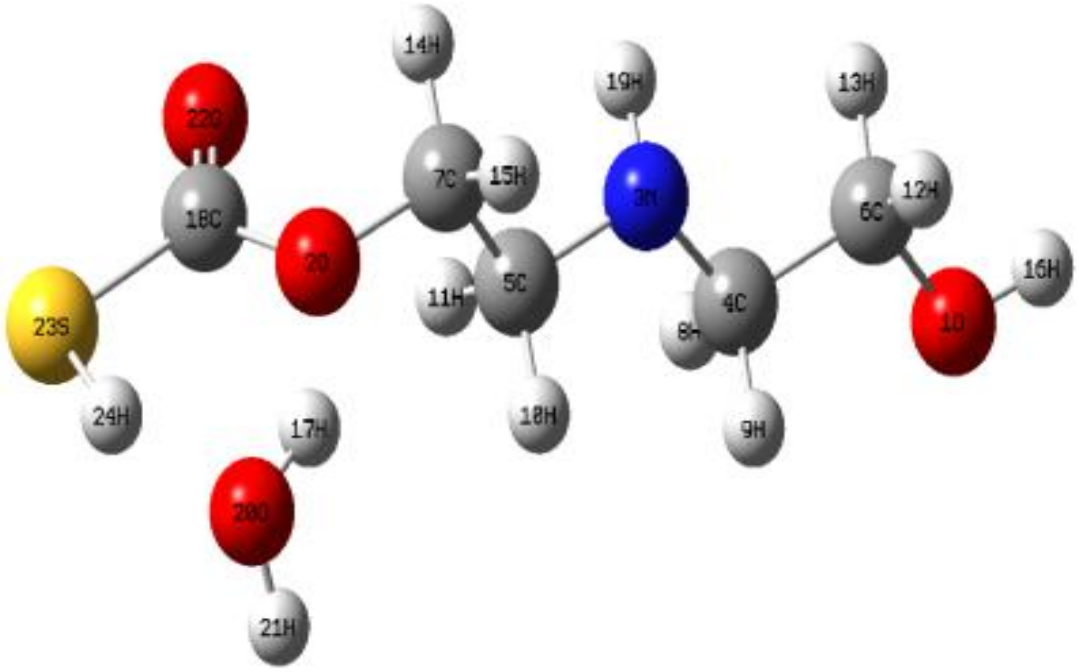

Figur 3.6 D. WDSCO P

Table 3.1 A. Bond lengths of DWOCS R, TS and P obtained from the B3LYP/6-311G(d) level calculations.

Bond Lengths (Å)	DWOCS-R	DWOCS-TS	DWOCS-P
N3-O1	3.673	3.692	3.685
C4-N3	1.460	1.492	1.461
C5-N3	1.459	1.487	1.467
C6-O1	1.425	1.422	1.437
C7-O2	1.423	1.418	1.421
H8-C4	1.103	1.092	1.090
H9-C4	1.095	1.092	1.090
H10-C5	1.098	1.094	1.089
H11-C5	1.104	1.092	1.093
H12-C6	1.099	1.097	1.095
H13-C6	1.100	1.097	1.095
H14-C7	1.093	1.093	1.093
H15-C7	1.098	1.096	1.095
H16-O1	0.963	0.963	0.963
H17-O2	0.964	0.964	0.964
C18-N3	3.417	1.528	1.369
H19-N3	1.020	1.311	3.420
H19-O20	2.07	1.208	0.96
O20-N3	3.053	2.453	2.754
H21-O20	0.962	0.962	0.973
H22-O20	0.965	1.267	1.758
H22-O23	2.145	1.17	0.985
O23-C18	1.160	1.277	1.332
S24-C18	1.565	1.651	1.677

In the reactant, C18-N3 distance is 3.417 Å which shows a weak interaction between amine and COS. But in the Ts, the distance decreases to 1.528 Å and in the product C18-N3 bond is formed with a length of 1.369 Å.

For the H19-O20, the distance is 2.07 Å in reactant which shows a weak interaction between amine and water. But in the Ts, the distance decreases to 1.208 Å and in the product H19-O20 bond is formed with a length of 0.96 Å.

The H22-O23 distance in the reactant is 2.145 Å which shows a weak interaction between water and COS. But in the Ts, the distance decreases to 1.17 Å and in the product H22-O23 bond is formed with a length of 0.985 Å.

Table 3.1 A. Bond angles of DWOCS R, TS and P obtained from the B3LYP/6-311G(d) level calculations.

Bond Angles (˚)	DWOCS-R	DWOCS-TS	DWOCS-P
N3-O1-O2	11.12	14.98	24.92
C4-N3-O1	21.35	19.36	21.86
C5-N3-O1	134.39	129.98	123.67
C6-O1-C4	37.67	38.99	37.73
C7-O2-O1	32.32	37.88	36.62
H8-C4-N3	113.19	107.26	110.96
H9-C4-N3	109.09	109.46	108.41
H10-C5-N3	108.54	108.97	108.44
H11-C5-N3	113.42	107.55	108.57
H12-C6-O1	111.44	111.26	110.47
H13-C6-O1	111.05	111.61	110.39
H14-C7-O2	105.68	105.87	106.01
H15-C7-O2	111.41	111.52	111.93
H16-O1-C6	108.49	108.63	109.36
H17-O2-O1	92.94	101.10	121.28
C18-N3-O1	104.10	102.17	111.27
H19-N3-O1	97.99	95.08	___
O20-N3-O1	105.58	94.44	___
H21-O20-N3	123.71	124.45	___
H22-O20-N3	85.86	68.72	___
O23-C1-N3	80.48	112.08	117.83
S24-C18-N3	101.15	120.39	123.89
S24-C18-O23	178.36	127.53	118.278
O20-O1-C6	___	___	87.73
H21-O20-O1	___	___	22.24
H22-O20-O1	___	___	91.95

The S24-C18-O23 bond angle in the reactant is 178.36 ˚ which is a linear. In the Ts, the bond angle becomes slightly bent and decreases to 127.53 ˚, and in the product S24-C18-O23 bond angle becomes bent with 118.278 ˚.

Table 3.1 A. Dihedral angles of DWOCS R, TS and P obtained from the B3LYP/6-311G(d) level calculations.

Dihedral Angles (˚)	DWOCS-R	DWOCS-TS	DWOCS-P
C4-N3-O1-O2	-1.06	23.32	-52.67
C5-N3-O1-C4	1.64	-13.31	78.11
C6-O1-C4-N3	-0.28	9.69	25.83
C7-O2-O1-C6	-9.04	4.24	90.38
H8-C4-N3-O1	-122.22	-113.34	-107.54
H9-C4-N3-O1	119.14	128.88	136.83
H10-C5-N3-O1	55.32	69.31	122.08
H11-C5-N3-O1	-62.80	-48.02	4.96
H12-C6-O1-C4	119.59	119.44	120.40
H13-C6-O1-C4	-119.98	-119.30	-119.94
H14-C7-O2-O1	118.59	110.78	76.69
H15-C7-O2-O1	-124.98	-132.24	-165.62
H16-O1-C6-C4	178.48	-175.29	-164.99
H17-O2-O1-C6	-129.31	-101.94	12.44
C18-N3-O1-C6	-33.03	-46.63	91.70
H19-N3-O1-C6	55.90	57.33	___
O20-N3-O1-C6	44.77	44.69	___
H21-O20-N3-O1	143.57	150.34	___
H22-O20-N3-O1	-108.56	-102.35	___
O23-C18-N3-O1	114.71	93.52	21.50
S24-C18-N3-O1	-65.42	-85.95	-157.74
O1-C6-C4-N3	179.83	-174.521	-164.459
C6-C4-N3-C5	-178.897	175.259	-98.53
C4-N3-C5-C7	175.786	-172.772	-92.22
N3-C5-C7-O2	173.865	178.09	179.8
S24-C18-O23-H22	___	___	-176.716

In reactant, Ts and product, the dihedral angels O1-C6-C4-N3, C6-C4-N3-C5 and C4-N3-C5-C7 are mostly rotate anticlockwise giving negative values. The N3-C5-C7-O2 dihedral angle rotates clockwise giving positive value. In the products S24-C18-O23-H22 dihedral angle rotates anticlockwise with a negative value.

Table 3.1 B. Bond lengths of DWSCO R, TS and P obtained from the B3LYP/6-311G(d) level calculations.

Bond Lengths (Å)	DWOCS-R	DWOCS-TS	DWOCS-P
N3-O1	3.684	3.696	3.698
C4-N3	1.487	1.492	1.455
C5-N3	1.486	1.489	1.471
C6-O1	1.423	1.423	1.437
C7-O2	1.419	1.419	1.422
H8-C4	1.093	1.092	1.092
H9-C4	1.090	1.093	1.088
H10-C5	1.092	1.095	1.092
H11-C5	1.093	1.092	1.092
H12-C6	1.096	1.097	1.095
H13-C6	1.098	1.097	1.095
H14-C7	1.092	1.093	1.093
H15-C7	1.095	1.096	1.095
H16-O1	0.963	0.963	0.963
H17-O2	0.964	0.964	0.964
O18-N3	2.404	2.347	2.268
C19-N3	1.73	1.53	1.37
C19-O18	1.193	1.202	1.213
S20-C19	1.679	1.747	1.818
H21-N3	1.032	1.369	1.360
H21-O22	1.82	1.157	--
O22-N3	2.842	2.489	2.800
H23-O22	0.962	0.964	0.962
H24-O22	0.978	1.268	0.973
H21-S20	2.77	2.72	1.359

In the reactant, C19-N3 distance is 1.73 Å, which decreases In the Ts, 1.53 Å and the bond starts forming, in the product the C19-N3 bond is formed with a length of 1.37 Å.

For the H21-O22, the distance in reactant is 1.82 Å which shows a weak interaction between amine and water. In the Ts, the distance decreases to 1.157 Å. In the product H21-S20 bond is formed with a length of 1.359 Å.

Table 3.1 B. Bond angles of DWSCO R, TS and P obtained from the B3LYP/6-311G(d) level calculations.

Bond Angles (˚)	DWOCS-R	DWOCS-TS	DWOCS-P
N3-O1-O2	14.79	15.81	33.29
C4-N3-O1	19.50	19.04	19.78
C5-N3-O1	130.68	128.45	120.32
C6-O1-C4	39.03	39.00	37.97
C7-O2-O1	38.26	39.29	31.50
H8-C4-N3	108.75	107.48	108.43
H9-C4-N3	107.77	109.55	110.59
H10-C5-N3	107.03	108.95	108.19
H11-C5-N3	109.02	107.86	108.48
H12-C6-O1	111.46	111.21	110.74
H13-C6-O1	111.63	111.54	110.13
H14-C7-O2	106.25	105.80	105.77
H15-C7-O2	111.72	111.47	111.77
H16-O1-C6	108.59	108.56	109.18
H17-O2-O1	103.57	99.98	133.50
O18-N3-O1	98.13	98.51	144.39
C19-O18-N3	42.76	35.44	30.91
S20-C19-O18	137.64	126.95	115.70
H21-N3-O1	95.23	95.40	104.48
O22-N3-O1	92.70	94.65	94.68
H23-O22-N3	132.85	120.13	115.90
H24-O22-N3	80.29	75.95	15.22

The S20-C19-O18 bond angle in the reactant is 137.64 ˚ which is slightly bent. In the Ts, the S20-C19-O18 bond angle decreases to 126.95 ˚ and in the product, S20-C19-O18 bond angle becomes bent with 115.70 ˚.

Table 3.1 B: dihedral angles of DWSCO R, TS and P obtained from the B3LYP/6-311G(d) level calculations.

Dihedral Angles (˚)	DWOCS-R	DWOCS-TS	DWOCS-P
C4-N3-O1-O2	27.47	21.77	113.67
C5-N3-O1-C4	-15.46	-13.01	-91.50
C6-O1-C4-N3	12.21	11.92	-11.90
C7-O2-O1-C6	0.04	1.87	-7.89
H8-C4-N3-O1	-112.90	-112.09	-128.86
H9-C4-N3-O1	129.62	130.43	114.89
H10-C5-N3-O1	68.73	65.95	161.25
H11-C5-N3-O1	-48.42	-51.24	44.33
H12-C6-O1-C4	119.55	119.59	119.92
H13-C6-O1-C4	-119.18	-119.36	-120.08
H14-C7-O2-O1	109.41	111.97	46.58
H15-C7-O2-O1	-133.50	-131.33	164.17
H16-O1-C6-C4	-175.19	-175.49	172.94
H17-O2-O1-C6	-103.16	-105.44	-51.79
O18-N3-O1-C6	-78.21	-76.70	-68.28
C19-O18-N3-O1	101.14	100.52	-33.75
S20-C19-O18-N3	179.79	179.74	179.81
H21-N3-O1-C6	60.25	60.14	-179.41
O22-N3-O1-C6	51.93	50.99	-64.42
H23-O22-N3-O1	150.78	149.84	127.23
H24-O22-N3-O1	-103.68	-103.09	-173.59
O1-C6-C4-N3	-173.07	-173.33	173.2
C6-C4-N3-C5	175.174	176.79	92.37
C4-N3-C5-C7	-175.1	-176.09	-100.37
N3-C5-C7-O2	173.97	175.53	179.85
O18-C19-S20-H21	___	___	-179.41

The dihedral angel O1-C6-C4-N3 rotates anticlockwise in the reactants and Ts, and clockwise at products. The dihedral angel C4-N3-C5-C7 rotates anticlockwise with negative values in all reaction steps. The dihedral angels C6-C4-N3-C5, N3-C5-C7-O2 are rotate clockwise with positive values in all reaction steps. In the products, dihedral angle O18-C19-S20-H21 rotates anticlockwise with a negative value.

Table 3.1 C. Bond lengths of WDOCS R, TS and P obtained from the B3LYP/6-311G(d) level calculations.

Bond Lengths (Å)	DWOCS-R	DWOCS-TS	DWOCS-P
N3-O1	3.672	3.669	3.669
C4-N3	1.460	1.462	1.462
C5-N3	1.460	1.459	1.459
C6-O1	1.424	1.423	1.422
C7-O2	1.416	1.443	1.447
H8-C4	1.103	1.102	1.102
H9-C4	1.094	1.094	1.094
H10-C5	1.096	1.096	1.095
H11-C5	1.104	1.101	1.100
H12-C6	1.098	1.098	1.098
H13-C6	1.102	1.101	1.101
H14-C7	1.095	1.090	1.090
H15-C7	1.098	1.091	1.090
H16-O1	0.963	0.963	0.963
H17-O2	0.973	1.306	2.421
C18-O2	3.109	1.529	1.355
H19-N3	1.017	1.017	1.017
O20-O2	2.802	2.370	2.905
H17-O20	1.86	1.30	0.964
H21-O20	0.965	1.046	1.693
H21-O23	2.15	1.51	0.993
H22-O20	0.962	0.965	0.963
O23-C18	1.161	1.235	1.313
S24-C18	1.563	1.656	1.654

In the reactant, C18-O2 distance is 3.109 Å which shows a weak interaction between oxygen of –OH group in amine and COS. But in the Ts, the distance decreases to 1.529 Å and in the product C18-O2 bond is formed with a length of 1.355 Å.

For the H17-O20, the distance is 1.86 Å in reactant which shows a weak interaction between hydrogen of –OH group in amine and water. But in the Ts, the distance decreases to 1.30 Å and in the product H17-O20 bond is formed with a length of 0.96 Å.

The H21-O23 distance in the reactant is 2.15 Å which shows a weak interaction between hydrogen of water and COS. But in the Ts, the distance decreases to 1.51 Å and in the product H21-O23 bond is formed with a length of 0.993 Å.

Table 3.1 C. Bond angles of WDOCS R, TS and P obtained from the B3LYP/6-311G(d) level calculations.

Bond Angles (˚)	DWOCS-R	DWOCS-TS	DWOCS-P
N3-O1-O2	11.29	11.13	11.31
C4-N3-O1	21.37	21.39	21.43
C5-N3-O1	134.89	135.02	135.07
C6-O1-C4	37.68	37.80	37.80
C7-O2-O1	32.86	31.99	32.04
H8-C4-N3	113.66	113.55	113.56
H9-C4-N3	108.49	108.58	108.57
H10-C5-N3	108.11	108.24	108.37
H11-C5-N3	113.40	113.86	113.76
H12-C6-O1	111.86	111.87	111.89
H13-C6-O1	110.90	110.97	110.98
H14-C7-O2	106.38	107.27	108.74
H15-C7-O2	111.87	106.76	105.22
H16-O1-C6	108.59	108.66	108.66
H17-O2-O1	92.56	118.59	112.67
C18-O2-O1	99.37	125.12	121.07
H19-N3-O1	99.16	98.91	98.98
O20-O2-O1	88.50	129.89	127.51
H21-O20-O2	91.35	75.17	48.29
H22-O20-O2	122.38	117.79	127.48
O23-C18-O2	82.61	108.52	110.38
S24-C18-O2	99.22	117.72	126.31
S24-C18-O23	178.16	133.67	123.30

The S24-C18-O23 bond angle in the reactant is 178.16 ˚ which is a linear. But in the Ts, the bond angle becomes slightly bent and decreases to 133.67 ˚ and in the product S24-C18-O23 bond angle becomes bent with 123.30 ˚.

Table 3.1 C. Dihedral angles of WDOCS R, TS and P obtained from the B3LYP/6-311G(d) level calculations.

Dihedral Angles (˚)	DWOCS-R	DWOCS-TS	DWOCS-P
C4-N3-O1-O2	-16.15	-19.91	-22.98
C5-N3-O1-C4	8.77	7.61	7.96
C6-O1-C4-N3	-0.81	-1.71	-1.86
C7-O2-O1-C6	4.20	-4.26	-3.29
H8-C4-N3-O1	-123.40	-123.75	-123.84
H9-C4-N3-O1	118.17	117.57	117.45
H10-C5-N3-O1	55.20	48.77	47.69
H11-C5-N3-O1	-62.54	-70.27	-71.40
H12-C6-O1-C4	119.64	119.58	119.56
H13-C6-O1-C4	-120.06	-120.00	-120.00
H14-C7-O2-O1	125.36	129.49	132.72
H15-C7-O2-O1	-117.83	-113.66	-110.06
H16-O1-C6-C4	-178.34	-179.57	-179.45
H17-O2-O1-C6	-116.35	-119.45	-124.73
C18-O2-O1-C6	152.48	94.51	95.54
H19-N3-O1-C6	59.39	57.61	57.51
O20-O2-O1-C6	-127.83	-127.53	-136.76
H21-O20-O2-O1	-89.60	-146.22	-140.31
H22-O20-O2-O1	22.19	-40.92	-44.93
O23-C18-O2-O1	71.83	146.22	142.90
O2-C7-C5-N3	-178.35	179.014	-179. 6
C7-C5-N3-C4	177.76	170.62	169.32
C5-N3-C4-C6	-173.71	-175.18	-175.0
N3-C4-C6-O1	179.51	178.966	178.87
S24-C18-O23-H21	___	___	-179.56

In reactants, Ts and products, the dihedral angel C5-N3-C4-C6, rotate anticlockwise giving negative values, but C7-C5-N3-C4 and N3-C4-C6-O1 dihedral angles, are rotate clockwise giving positive values. In the products S24-C18-O23-H21 dihedral angle rotates anticlockwise with a negative value.

Table 3.1 D. Bond lengths of WDSCO R, TS and P obtained from the B3LYP/6-311G(d) level calculations.

Bond Lengths (Å)	DWOCS-R	DWOCS-TS	DWOCS-P
N3-O1	3.672	3.669	3.669
C4-N3	1.460	1.462	1.462
C5-N3	1.460	1.459	1.459
C6-O1	1.424	1.422	1.422
C7-O2	1.416	1.447	1.447
H8-C4	1.103	1.102	1.102
H9-C4	1.095	1.094	1.094
H10-C5	1.097	1.095	1.095
H11-C5	1.104	1.101	1.101
H12-C6	1.098	1.098	1.098
H13-C6	1.102	1.102	1.102
H14-C7	1.095	1.090	1.090
H15-C7	1.099	1.091	1.091
H16-O1	0.963	0.963	0.963
H17-O2	0.972	1.254	1.254
C18-O2	2.971	1.540	1.36
H19-N3	1.017	1.017	1.017
O20-O2	2.810	2.381	2.381
H21-20	0.963	0.966	0.966
H17-O20	1.85	1.25	0.966
H22-C18	0.962	___	___
O23-C18	1.154	___	___
H24-S23	___	1.94	1.36
S24-C18	1.575	___	___
O22-C18	___	1.189	1.189
H24-O18	___	1.052	___
H24-S23	___	___	1.052

In the reactant, C18-O2 distance is 2.97 Å. In the Ts, the distance decreases to 1.54 Å and the bond starts forming, in the product the C18-O2 bond is formed with a length of 1.36 Å.

For the H17-O20, the distance in reactant is 1.85 Å which shows a weak interaction between amine and water. In the Ts, the distance decreases to 1.25 Å. In the product H17-O20 bond is formed with a length of 0.966 Å.

In the product the bond H24-S23 is formed with a length of 1.052 Å.

Table 3.1 D. Bond angles of WDSCO R, TS and P obtained from the B3LYP/6-311G(d) level calculations.

Bond Angles (˚)	DWOCS-R	DWOCS-TS	DWOCS-P
N3-O1-O2	11.25	11.33	11.53
C4-N3-O1	21.38	21.41	21.38
C5-N3-O1	134.93	135.08	135.06
C6-O1-C4	37.67	37.82	37.84
C7-O2-O1	32.77	32.17	32.28
H8-C4-N3	113.70	113.53	113.54
H9-C4-N3	108.51	108.57	108.57
H10-C5-N3	108.11	108.31	108.37
H11-C5-N3	113.39	113.91	113.73
H12-C6-O1	111.84	111.91	111.91
H13-C6-O1	110.90	110.98	110.98
H14-C7-O2	106.26	107.42	108.56
H15-C7-O2	111.89	106.94	105.28
H16-O1-C6	108.57	108.69	108.70
H17-O2-O1	92.32	121.37	113.75
C18-O2-O1	101.94	119.97	115.47
H19-N3-O1	99.16	98.92	98.70
H21-O20-O2	101.36	115.76	107.66
O23-C18-O2	84.97	___	___
S24-C18-O2	97.55	___	___
S23-C18-O2	___	111.71	112.79
S23-C18-O22	177.46	133.97	122.87
H24-O20-O2	___	80.63	___
H24-S23-C18	___	___	96.84

The S24-C18-O22 bond angle in the reactant is 177.46 ˚ which is a linear. But in the Ts, the bond angle becomes slightly bent and decreases to 133.97 ˚ and in the product S24-C18-O23 bond angle becomes bent with 122.87 ˚.

Table 3.1 D. Dihedral angles of WDSCO R, TS and P obtained from the B3LYP/6-311G(d) level calculations.

Dihedral angles (˚)	DWOCS-R	DWOCS-TS	DWOCS-P
C4-N3-O1-O2	-16.13	-22.69	-23.48
C5-N3-O1-C4	8.72	8.24	7.22
C6-O1-C4-N3	-1.36	-1.63	-0.94
C7-O2-O1-C6	3.23	-2.35	-0.99
H10-C5-N3-O1	55.08	48.07	47.73
H11-C5-N3-O1	-62.91	-70.96	-71.28
H13-C6-O1-C4	-120.06	-120.01	-119.98
H16-O1-C6-C4	-178.93	-179.26	-178.70
H17-O2-O1-C6	-118.45	-108.08	-112.51
C18-O2-O1-C6	132.61	93.37	97.50
H19-N3-O1-C6	58.68	57.93	58.14
O20-O2-O1-C6	-127.32	-113.48	-122.03
O23-C18-O2-O1	-63.84	___	___
S24-C18-O2-O1	115.85	___	___
S23-C18-O2-O1	___	151.68	144.44
H24-O20-O2-O1	___	-152.73	___
H24-S23-C18-O2	___	___	0.85
O1-C6-C4-N3	179.18	179.01	179.43
C6-C4-N3-C5	-174.09	-174.64	-175
C4-N3-C5-C7	177.55	170	168.96
N3-C5-C7-O2	-178.57	-179.43	-177.98
O22-C18-S23-H24	___	___	-179.05

The dihedral angels C6-C4-N3-C5 and N3-C5-C7-O2 rotate anticlockwise with negative values, and the dihedral angels O1-C6-C4-N3, C4-N3-C5-C7 are rotate clockwise with positive values. In the products, dihedral angle O22-C18-S23-H24 rotates anticlockwise with a negative value.

3.4 INFRARED (IR) SPECTRUM OF THE REACTION SYSTEMS

IR spectra for the reactants, transition states and products of all four reaction systems are calculated on the optimized geometries at the B3LYP/6-311G(d) level of theory and represented in the figures 3.7 A-D.

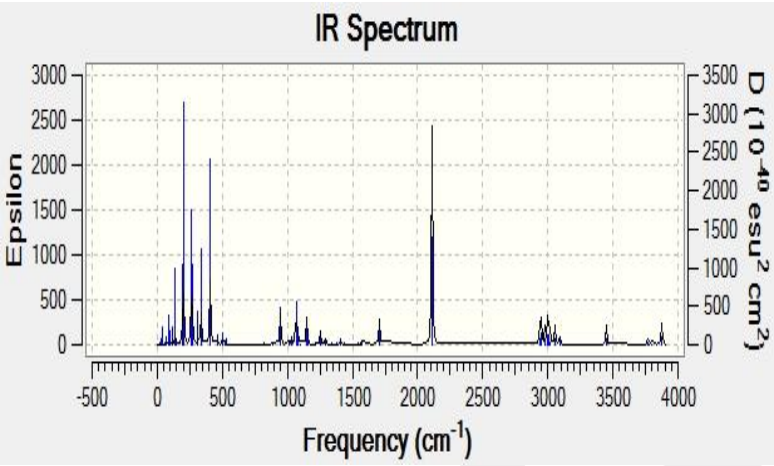

Figure 3.7 A: DWOCS reactants IR spectrum

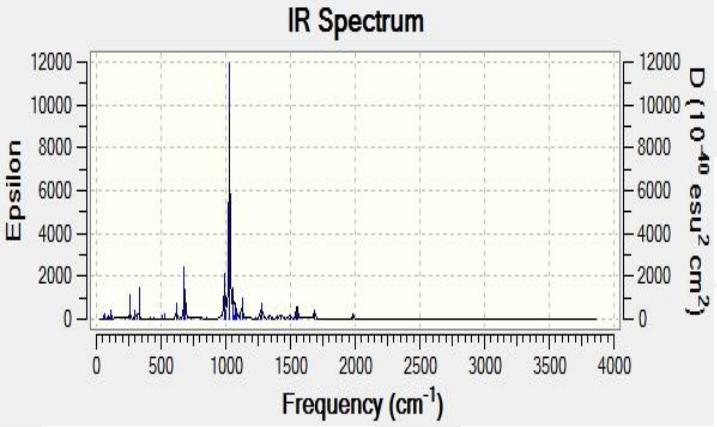

Figure 3.7 A: DWOCS transition state IR spectrum

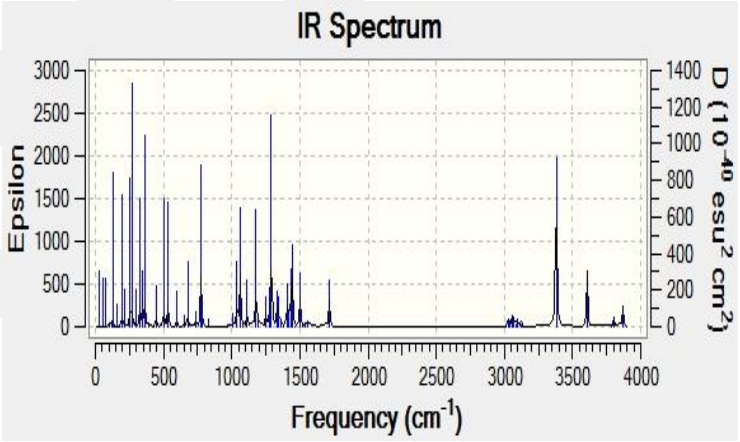

Figure 3.7 A: DWOCS products IR spectrum

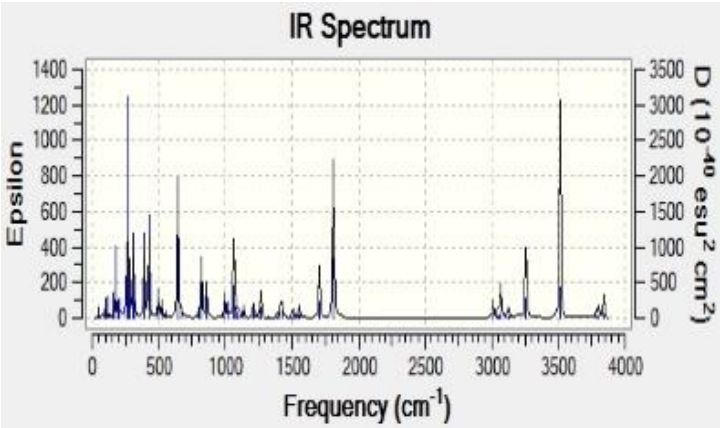

Figure 3.7 B: DWSCO reactants IR spectrum

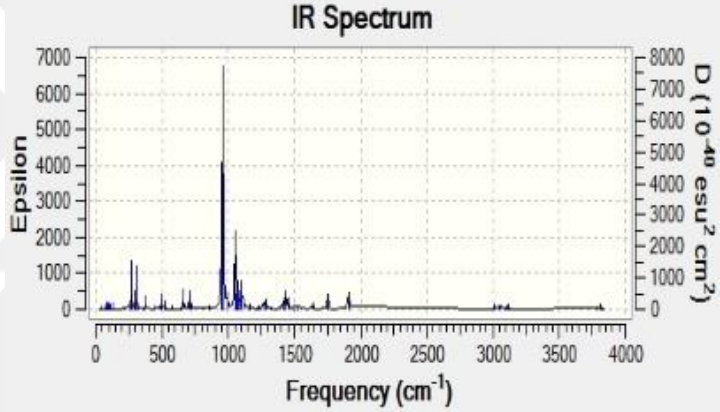

Figure 3.7 B: DWSCO transition state IR spectrum

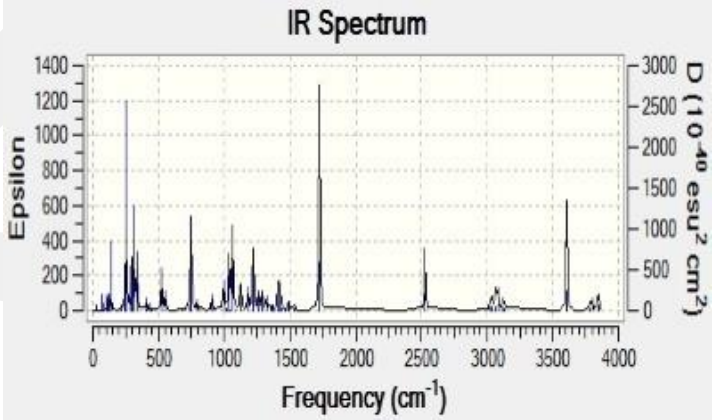

Figure 3.7 B: DWSCO products IR spectrum

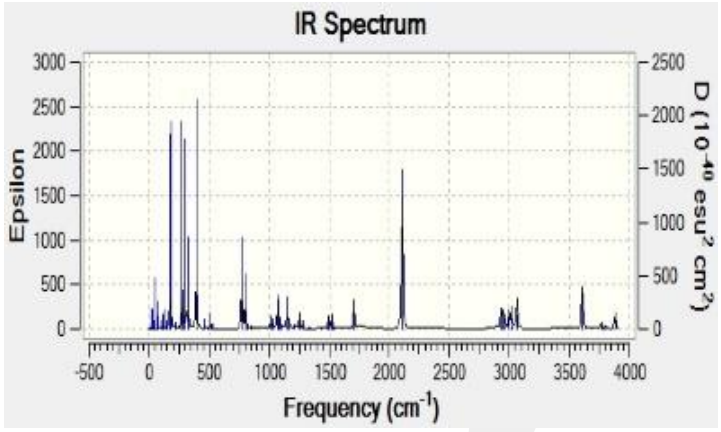

Figure 3.7 C: WDOCS reactants IR spectrum

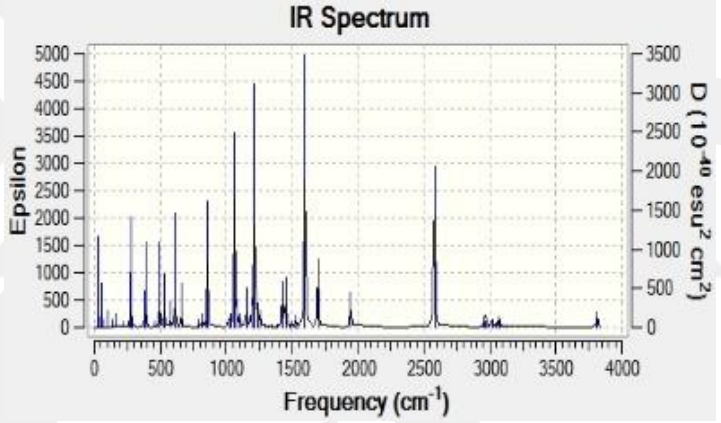

Figure 3.7 C: WDOCS transition state IR spectrum

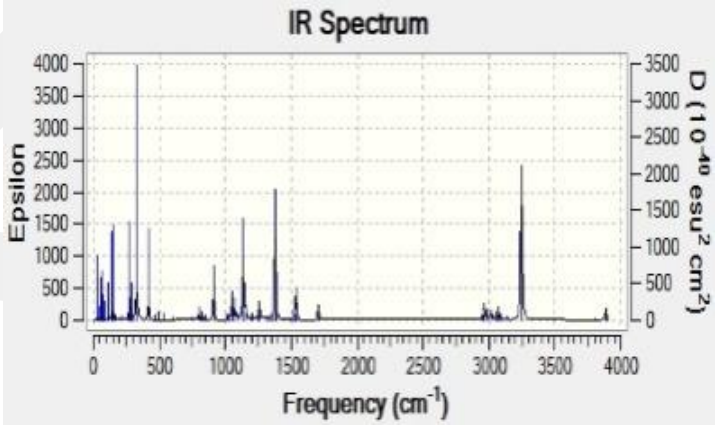

Figure 3.7 C: WDOCS products IR spectrum

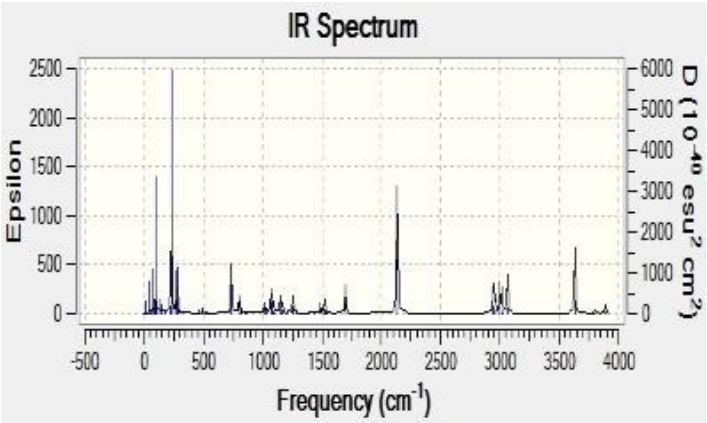

Figure 3.7 D: WDSCO reactants IR spectrum

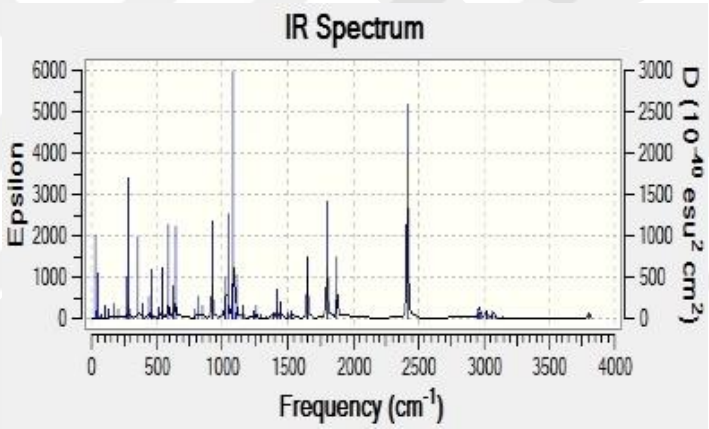

Figure 3.7 D: WDSCO transition state IR spectrum

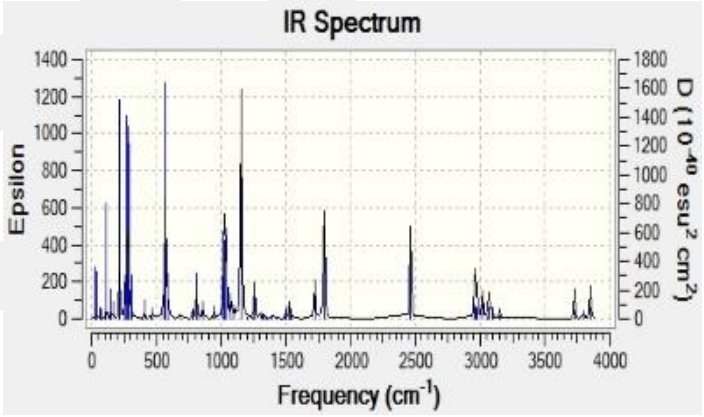

Figure 3.7 D: WDSCO products IR spectrum

3.5 IMAGINARY FREQUENCY OF THE TRANSITION STATE

The transition state of the vibrational spectrum distinguished with an imaginary frequency, which has a negative force constant.

This property said that the energy has a maximum value in one nuclear space configuration direction and minimum values in all else directions. Imaginary frequency value for all our transition state files as shown in next table. Intrinsic reaction coordinate (IRC) calculations on transition state structures either yield reactants or products.

Table 3.2 imaginary frequency values of transition state files

TS files	Imaginary frequency value
DWOCS_TS	-1573.86
DWSCO_TS	-1467.94
WDOCS_TS	-898.54
WDSCO_TS	-944.38

3.6 THERMOCHEMISTRY CALCULATIONS

Thermochemistry data obtained from B3LYP/6-311G(d), at standard conditions of 298 K temperature and 1 atm pressure, these data are important as they represent the energy calculations, which can be used to determine the standard free energy of activation ($\Delta^{\ddagger}G^{\circ}$), standard free energy of reaction (ΔG°_{rxn}), equilibrium constant (K_{eq}) and reaction rate constant (k).

3.6.1 Calculation of the reaction equilibrium constant (K_{eq}).

K_{eq} is calculated for the four mechanisms, as shown in tables 3.4 A-D at the B3LYP/6-311G(d) level of theory.

3.6.1.1 First mechanism: DEA(H of N)+Water+OCS

Table 3.3 A. Standard free energy of reaction and Equilibrium constant for the first mechanism, DWOCS.

hartree	kcal/mol	kJ/mol
1	627.503	2625.5

$\Delta G°_{rxn}$=	$G_{products} - G_{Reactants}$	
$\Delta G°_{rxn}$=	$G_P - G_R$	
$\Delta G°_{rxn}$=	0.019911	hartrees
$\Delta G°_{rxn}$=	12.49421223	kcal/mol
$\Delta G°_{rxn}$=	12494.21223	cal/mol

equilibrium constant K_{eq} =		$\exp(-\Delta G°_{rxn}/RT)$	
gas constant R	=	1.987	cal/mol. K
Temperature T	=	298.15	K
K_{eq}	=	6.930×10^{-10}	

Equilibrium constants (K_{eq}) for second to fourth mechanisms are calculated following the same procedure given in section 3.6.1.1.

3.6.1.2 Second mechanism: DEA(H of N)+Water+SCO

Table 3.3 B. Standard free energy of reaction and Equilibrium constant for the second mechanism DWSCO

$\Delta G°_{rxn}$=	$G_{products} - G_{reactants}$	
$\Delta G°_{rxn}$=	$G_P – G_R$	
$\Delta G°_{rxn}$=	-0.009693	Hartrees
$\Delta G°_{rxn}$=	-6.082386579	kcal/mol
$\Delta G°_{rxn}$=	-6082.386579	cal/mol
K_{eq} =	28765.94	

3.6.1.3 Third mechanism: DEA(H of OH)+Water+OCS

Table 3.3 C. Standard free energy of reaction and Equilibrium constant for the third mechanism WDOCS

$\Delta G°_{rxn}$=	$G_{products} - G_{reactants}$	
$\Delta G°_{rxn}$=	$G_P – G_R$	
$\Delta G°_{rxn}$=	0.022396	hartrees
$\Delta G°_{rxn}$=	14.05355719	kcal/mol
$\Delta G°_{rxn}$=	14053.55719	cal/mol
K_{eq} =	$4.984x10^{-11}$	

3.6.1.4 Fourth mechanism: DEA(H of OH)+Water+SCO

Table 3.3 D. Standard free energy of reaction and Equilibrium constant for the forth mechanism WDSCO

$\Delta G°_{rxn}$=	$G_{products} - G_{reactants}$	
$\Delta G°_{rxn}$=	$G_P – G_R$	
$\Delta G°_{rxn}$=	0.008686	hartrees
$\Delta G°_{rxn}$=	5.450491058	kcal/mol
$\Delta G°_{rxn}$=	5450.491058	cal/mol
K_{eq} =	$1.010x10^{-04}$	

3.6.2 Calculation of reaction rate constant (k).

Reaction rate constant k values are calculated following the procedure postulated by Eyring [34, 49, 50]. This postulation states that the specific reaction rate constant for a reaction of any order can be generalized in the following equation.

$$k_i = c\left(\frac{F_a}{F_n}\right)\left(\frac{\bar{p}}{m^*}\right) = c\left(\frac{f_a^{'}}{F_n}\right)\left(\frac{kT}{h}\right)e^{\frac{E_0}{kT}} \qquad (1)$$

Where F_a partition function for the activated state, F_n is the same quantity for the normal state, $f_a^{'}$ partition function of the activated complex, the factor $\left(\frac{kT}{h}\right)e^{\frac{E_0}{kT}}$ is the partition function for normal coordinate, $\left(\frac{\bar{p}}{m^*}\right)$ average velocity, E_0 difference in energy between initial substances and activated state at the absolute zero, the factor c is the average numbers of crossings required for each complex, h is blank's constant and T is temperature.

Reaction rate constants for the four reaction mecahnisms are calculated using the standard free energy of activations and Eyring equation. The results are given in tables 3.5 A-D.

3.6.2.1 First mechanism: DEA(H of N)+Water+OCS

Table 3.4 A. Standard free energy of activation and Reaction rate constant for the first mechanism DWOCS

Standard free energy of activation $\Delta^{\ddagger}\mathbf{G}^{\circ} = G_{TS} - G_R$		
$\Delta^{\ddagger}\mathbf{G}^{\circ}$ =	0.049285	Hartrees
=	30.92648536	kcal/mol
=	129.3977675	kJ/mol
k =	1.326×10^{-10}	s^{-1}

3.6.2.2 Second mechanism: DEA(H of N)+Water+SCO

Table 3.4 B. Standard free energy of activation and Reaction rate constant for the second mechanism DWSCO.

Standard free energy of activation $\Delta^{\ddagger}\mathbf{G}^{\circ} = G_{TS} - G_R$		
$\Delta^{\ddagger}\mathbf{G}^{\circ}$ =	0.025700	Hartrees
=	16.1268271	kcal/mol
=	67.47535	kJ/mol
K =	9.363415071	s^{-1}

3.6.2.3 Third mechanism: DEA(H of OH)+Water+OCS

Table 3.4 C. Standard free energy of activation and Reaction rate constant for the third mechanism WDOCS.

Standard free energy of activation $\Delta^{\ddagger}\mathbf{G}^{\circ} = G_{TS} - G_R$		
$\Delta^{\ddagger}\mathbf{G}^{\circ}$ =	0.053233	hartrees
=	33.4038672	kcal/mol
=	139.7632415	kJ/mol
k =	2.025×10^{-12}	s^{-1}

3.6.2.4 Fourth mechanism: DEA(H of OH)+Water+SCO

Table 3.4 D. Standard free energy of activation and Reaction rate constant for the fourth mechanism WDSCO.

Standard free energy of activation $\Delta^{\ddagger}\mathbf{G}^{\circ} = G_{TS} - G_R$		
$\Delta^{\ddagger}\mathbf{G}^{\circ}$ =	0.041471	hartrees
=	26.02317691	kcal/mol
=	108.8821105	kJ/mol
k =	5.211×10^{-07}	s^{-1}

3.7 COMPARISON WITH EXPERIMENTS

This part of the investigation will be dedicated to compare the Standard free energy of activation $\Delta G^{\ddagger}$, and reaction rate constant (k) calculated in 3.6.2 section, with the experimental activation energies (E_a) and reaction rate constant (k) obtained from the literature as shown in table 3.6.

Table 3.5 comparison of Ea and k of present work with literature.

Reference / Data	amine conc. (mol/m^3)	Temp. (K)	Rate constant K_{app} (s-1)	Standard free energy of activation $\Delta^{\ddagger}G^{\circ}$ (kcal/mol)
Alper, E. and W. Bouhamra. (1993) [18]	100 - 1500	298	5.069	--
Littel, R., et al. (1992) [17]	1000	283	2.04*	11.843*
Littel, R., et al. (1992) [17]	1000	303	7.6	11.843*
M.M. Sharma. (1965) [15]	1000	298	11	--
Hinderaker, G. and O. C. Sandall (2000) [3]	959	298	14.3	12.5
Amararene, F. and C. Bouallou (2004)[4]	1433	313	28.3	11.5
DWOCS**	--	298.15	$1.326x10^{-10}$	30.93
DWSCO**	--	298.15	9.36	16.13
WDOCS**	--	298.15	$2x10^{-12}$	33.40
WDSCO**	--	298.15	$5.2x10^{-7}$	26.02

* Obtained after extrapolating data.

** This study. All values obtained from the B3LYP/6-311G(d) calculations.

The comparison in the above table performed using experimental data of reaction rate constant and activation energy established from five studies conducted on this reaction COS/DEA/Water, compared with our theoretical data of reaction rate constant and free energy of activation obtained from the B3LYP/6-311G(d) calculations for the same reaction.

The experimental values of reaction rate constant ranges bewteen 2.04 to 28.3 s^{-1}, taking in consideration the difference in temperature and concentration between different studies.

The theoretical values of reaction rate constant of first DWOCS, third WDOCS and fourth WDSCO mechanisms ranges between $2x10^{-12}$ to $5.2x10^{-7}$ s^{-1}.

In the second DWSCO mechanism, the theoretical value of reaction rate constant which is 9.36 s^{-1}, can be considered much closer to the experimental values, especially with Sharma. (1965) [15] reaction rate constant value which is 11 s^{-1}, of the same reaction COS/DEA/Water.

CHAPTER 4

CONCLUSION

In this study a theoretical investigation proceeded to study the carbonyl sulfide (COS) absorption and capturing by aqueous diethanolamine (DEA) solution.

Theoretical calculations proceeded using Gaussian software to get structural, energetic and reaction kinetics data with an electron correlation method, i.e., a Density Functional Theory methodology at the B3LYP/6-311G(d) level of theory.

The termolecular COS/DEA/WATER mechanism was applied investigated study taking in to accountof four types of proton transfer paths:

- DWOCS: transfer of proton of nitrogen to water and transfer of proton from water to the oxygen atom of O=C=S.
- DWSCO: transfer of proton of nitrogen to water and transfer of proton from water to the sulfur atom of S=C=O
- WDOCS: transfer of proton of OH in amine to water and transfer of proton from water to the oxygen atom of O=C=S
- WDSCO: transfer of proton of OH in amine to water and transfer of proton from water to the sulfur atom of S=C=O.

All computed properties for the four suggested reaction mechanisms were done for the reactants, transition states and products.

The study starts with the steps by optimizing the molecules geometrically which leads to the geometries shown in figures 3.2 A, B and C, figurs 3.3 A, B and C, figures 3.4 A, B and C and figures 3.5 A, B and C.

The distances between atoms, S=C=O or O=C=S angles and dihedral angles was calculated by DFT methodology in each coordinate of reactions, i.e., reactants, transition states and products for the four mechanism, as shown in Tables 3.1 A, B, C and D.

Then calculations were performed to obtain vibrational frequencies and IR Spectra of the four reaction systems, as shown in the plots in Figure 3.7 A - D.

The imaginary frequency values of the transition state structures of all the four reaction mechanisms obtained from the DFT calculations are shown in Table 3.2. It needs to be noted that intrinsic reaction coordinate calculations on these structures yield either reactants or products of each system.

Thermochemistry data were also obtained, these are important as they represent the energy calculations, these calculations used in this study to determine the standard free energy of activation and reaction, equilibrium constant and reaction rate constant.

The equilibrium constant (Keq), reaction rate constant (k), standard free energy of reaction and standard free energy of activation values of the studied four reaction mechanisms are shown in tables 3.3 and 3.4.

The last part was dedicated to make a comparison between theoretical data and experimental data for activation energies and reaction rate constants. The result of this comparison is shown in Table 3.5. Our findings suggest that the second reaction mechanism (DWSCO: transfer of proton of nitrogen to water and transfer of proton from water to the sulfur atom of S=C=O) is the most possible mechanism in the absorption of carbonyl sulfide by the aqueous solution of diethanolamine, since our results agree very well with the experimental data for this mechanism.

References

1. Elliott, S., E. Lu, and F.S. Rowland, *Rates and mechanisms for the hydrolysis of carbonyl sulfide in natural waters.* Environmental science & technology, 1989. **23**(4): p. 458-461.

2. Ernst, W.R., M.S. Chen, and D.L. Mitchell, *Hydrolysis of carbonyl sulfide: comparison to reactions of isocyanates.* The Canadian Journal of Chemical Engineering, 1990. **68**(2): p. 319-323.

3. Hinderaker, G. and O.C. Sandall, *Absorption of carbonyl sulfide in aqueous diethanolamine.* Chemical engineering science, 2000. **55**(23): p. 5813-5818.

4. Amararene, F. and C. Bouallou, *Kinetics of carbonyl sulfide (COS) absorption with aqueous solutions of diethanolamine and methyldiethanolamine.* Industrial & engineering chemistry research, 2004. **43**(19): p. 6136-6141.

5. Svoronos, P.D. and T.J. Bruno, *Carbonyl sulfide: a review of its chemistry and properties.* Industrial & engineering chemistry research, 2002. **41**(22): p. 5321-5336.

6. Vaidya, P.D. and E.Y. Kenig, *Kinetics of carbonyl sulfide reaction with alkanolamines: A review.* Chemical engineering journal, 2009. **148**(2): p. 207-211.

7. Hanst, P.L., et al., *Infrared measurement of fluorocarbons, carbon tetrachloride, carbonyl sulfide, and other atmospheric trace gases.* Journal of the Air Pollution Control Association, 1975. **25**(12): p. 1220-1226.

8. Adams, D., et al., *Preliminary measurements of biogenic sulfur-containing gas emissions from soils.* Journal of the Air Pollution Control Association, 1979. **29**(4): p. 380-383.

9. Watts, S.F., *The mass budgets of carbonyl sulfide, dimethyl sulfide, carbon disulfide and hydrogen sulfide.* Atmospheric Environment, 2000. **34**(5): p. 761-779.

10. Khalil, M. and R. Rasmussen, *Global sources, lifetimes and mass balances of carbonyl sulfide (OCS) and carbon disulfide (CS2) in the earth's atmosphere.* Atmospheric Environment (1967), 1984. **18**(9): p. 1805-1813.

11. Hewitt, C.N. and B.M. Davison, *The lifetimes of organosulphur compounds in the troposphere.* Applied organometallic chemistry, 1988. **2**(5): p. 407-415.

12. Chin, M. and D. Davis, *Global sources and sinks of OCS and CS2 and their distributions.* Global Biogeochemical Cycles, 1993. **7**(2): p. 321-337.

13. Gosselin, R.E., R.P. Smith, and H.C. Hodge, *Clinical toxicology of commercial products*. 1984: Williams & Wilkins.

14. Houriet, R. and D. Louvier, *Emission of toxic sulfur gases from polymers coming in contact with food products and with infants.* Analusis, 1999. **27**(4): p. 369-372.

15. Sharma, M., *Kinetics of reactions of carbonyl sulphide and carbon dioxide with amines and catalysis by Brönsted bases of the hydrolysis of COS.* Transactions of the Faraday Society, 1965. **61**: p. 681-688.

16. da Silva, E.F., *Computational chemistry study of solvents for carbon dioxide absorption (Doctoral dissertation).* 2005.

17. Littel, R., G. Versteeg, and W. Van Swaaij, *Kinetics of COS with primary and secondary amines in aqueous solutions.* AIChE journal, 1992. **38**(2): p. 244-250.

18. Alper, E. and W. Bouhamra, *Kinetics and mechanism of the reaction between carbonyl sulphide and primary and secondary amines in aqueous solutions.* DOGA TURKISH JOURNAL OF CHEMISTRY, 1993. **17**: p. 7-7.

19. Singh, M. and J.A. Bullin, *Determination of rate constants for the reaction between diglycolamine and carbonyl sulphide.* Gas Separation & Purification, 1988. **2**(3): p. 131-137.

20. Al-Ghawas, H.A., G. Ruiz-Ibanez, and O.C. Sandall, *Absorption of carbonyl sulfide in aqueous methyldiethanolamine.* Chemical engineering science, 1989. **44**(3): p. 631-639.

21. Littel, R.J., G.F. Versteeg, and W.P. Van Swaaij, *Kinetic study of COS with tertiary alkanolamine solutions. 1. Experiments in an intensely stirred batch reactor.* Industrial & engineering chemistry research, 1992. **31**(5): p. 1262-1269.

22. Littel, R.J., G.F. Versteeg, and W.P. Van Swaaij, *Kinetic study of COS with tertiary alkanolamine solutions. 2. Modeling and experiments in a stirred cell reactor.* Industrial & engineering chemistry research, 1992. **31**(5): p. 1269-1274.

23. Alper, E. and W. Bouhamra, *Reaction kinetics of carbonyl sulfide with aqueous ethylenediamine and diethylenetriamine.* Gas separation & purification, 1994. **8**(4): p. 237-240.

24. Alper, E. *Reaction kinetics of carbonyl sulfide with aqueous diglycolamine by the stopped flow technique*. in *Gas Processing Fundamentals I, AIChE Spring National Meeting, Houston*. 1989.

25. Sada, E., H. Kumazawa, and Z. Han, *Kinetics of reaction between carbon dioxide and ethylenediamine in nonaqueous solvents.* The Chemical Engineering Journal, 1985. **31**(2): p. 109-115.

26. Crooks, J.E. and J.P. Donnellan, *Kinetics and mechanism of the reaction between carbon dioxide and amines in aqueous solution.* Journal of the Chemical Society, Perkin Transactions 2, 1989(4): p. 331-333.

27. Ismael, M., et al., *A DFT study on the carbamates formation through the absorption of CO 2 by AMP.* International Journal of Greenhouse Gas Control, 2009. **3**(5): p. 612-616.

28. Da Silva, E.F. and H.F. Svendsen, *Computational chemistry study of reactions, equilibrium and kinetics of chemical CO 2 absorption* International Journal of Greenhouse Gas Control, 2007. **1**(2): p. 151-157.

29. Cramer, C.J., *Essentials of computational chemistry: theories and models*. 2013: John Wiley & Sons.

30. Hehre, W., A. Shusterman, and J. Nelson, *The Molecular Modeling Workbook for Organic Chemistry, Wavefunction.* Inc., Irvine, CA, 1998. **92612**.

31. Jensen, F., *Introduction to computational chemistry*. 2016: John wiley & sons.

32. Parr, R.G. and W. Yang, *Density-functional theory of atoms and molecules*. 1989, Oxford University Press New York, NY, USA.

33. Koch, W. and M.C. Holthausen, *A chemist's guide to density functional theory*. 2015: John Wiley & Sons.

34. Withnall, R., et al., *Computational chemistry using modern electronic structure methods.* J. Chem. Educ, 2007. **84**(8): p. 1364.

35. Hohenberg, P. and W. Kohn, *Inhomogeneous electron gas.* Physical review, 1964. **136**(3B): p. B864.

36. Kohn, W. and L.J. Sham, *Self-consistent equations including exchange and correlation effects.* Physical review, 1965. **140**(4A): p. A1133.

37. Jacobsen, H. and L. Cavallo, *Directions for Use of Density Functional Theory: A Short Instruction Manual for Chemists*, in *Handbook of Computational Chemistry*. 2012, Springer. p. 95-133.

38. Whitfield, J.D., *At the intersection of quantum computing and quantum chemistry (Doctoral dissertation)*. 2011, Harvard University Cambridge, Massachusetts.

39. Hehre, W.J., R.F. Stewart, and J.A. Pople, *self-consistent molecular-orbital methods. i. use of gaussian expansions of Slater-type atomic orbitals.* The Journal of Chemical Physics, 1969. **51**(6): p. 2657-2664.

40. Pople, J.A., D.P. Santry, and G.A. Segal, *Approximate self-consistent molecular orbital theory. I. Invariant procedures.* The Journal of Chemical Physics, 1965. **43**(10): p. S129-S135.

41. Pople, J.A. and G.A. Segal, *Approximate Self-Consistent Molecular Orbital Theory. II. Calculations with Complete Neglect of Differential Overlap.* The Journal of Chemical Physics, 1965. **43**(10): p. S136-S151.

42. McLean, A. and G. Chandler, *Contracted Gaussian basis sets for molecular calculations. I. Second row atoms, Z= 11–18.* The Journal of Chemical Physics, 1980. **72**(10): p. 5639-5648.

43. Dunning Jr, T.H., *Gaussian basis sets for use in correlated molecular calculations. I. The atoms boron through neon and hydrogen.* The Journal of chemical physics, 1989. **90**(2): p. 1007-1023.

44. Becke, A.D., *Density-functional exchange-energy approximation with correct asymptotic behavior.* Physical review A, 1988. **38**(6): p. 3098.

45. Lee, C., W. Yang, and R.G. Parr, *Development of the Colle-Salvetti correlation-energy formula into a functional of the electron density.* Physical review B, 1988. **37**(2): p. 785.

46. Becke, A.D., *Density-functional thermochemistry. III. The role of exact exchange.* The Journal of chemical physics, 1993. **98**(7): p. 5648-5652.

47. Perdew, J.P., P. Ziesche, and H. Eschrig, *Electronic structure of solids' 91*. Vol. 11. 1991: Akademie Verlag, Berlin.

48. M. J. Frisch, G.W.T., H. B. Schlegel, G. E. Scuseria, , et al., *Gaussian 09, revision D. 01*. 2009, Gaussian, Inc., Wallingford CT.

49. Cuevas, J.C., *Introduction to density functional theory*. Universität Karlsruhe, Germany, 2010.

50. Eyring, H., *The activated complex in chemical reactions.* The Journal of Chemical Physics, 1935. **3**(2): p. 107-115.